

# CiteVQA: Benchmarking Evidence Attribution for Trustworthy Document Intelligence

Dongsheng Ma<sup>1,2\*</sup>, Jiayu Li<sup>2\*</sup>, Zhengren Wang<sup>1,2\*</sup>, Yijie Wang<sup>2</sup>, Jiahao Kong<sup>2</sup>, Weijun Zeng<sup>1,2</sup>, Jutao Xiao<sup>2</sup>, Jie Yang<sup>2</sup>, Wentao Zhang<sup>1</sup> , Bin Wang<sup>2</sup> , Conghui He<sup>2</sup> 

<sup>1</sup>Peking University, <sup>2</sup>Shanghai Artificial Intelligence Laboratory  
wzr@stu.pku.edu.cn, wentao.zhang@pku.edu.cn, {wangbin, heconghui}@pjlab.org.cn

Multimodal Large Language Models (MLLMs) have significantly advanced document understanding, yet current Doc-VQA evaluations score only the final answer and leave the supporting evidence unchecked. This answer-only approach masks a critical failure mode: a model can land on the correct answer while grounding it in the wrong passage—a critical risk in high-stakes domains like law, finance, and medicine, where every conclusion must be traceable to a specific source region. To address this, we introduce **CiteVQA**, a benchmark that requires models to return *element-level* bounding-box citations alongside each answer, evaluating both jointly. CiteVQA comprises 1,897 questions across 711 PDFs spanning seven domains and two languages, averaging 40.6 pages per document. To ensure fidelity and scalability, the ground-truth citations are generated by an automated pipeline—which identifies crucial evidence via masking ablation—and are subsequently validated through expert review. At the core of our evaluation is Strict Attributed Accuracy (SAA), which credits a prediction only when the answer and the cited region are both correct. Auditing 20 MLLMs reveals a pervasive **Attribution Hallucination**: models frequently produce the right answer while citing the wrong region. The strongest system (Gemini-3.1-Pro-Preview) achieves an SAA of only 76.0, and the strongest open-source MLLM reaches just 22.5. Ultimately, towards trustworthy document intelligence, CiteVQA exposes a reliability gap that answer-only evaluations overlook, providing the instrumentation needed to close it. Our repository is available at <https://github.com/pendatalab/CiteVQA>.

\* Equal contribution  Corresponding author

## 1 Introduction

In recent years, Multimodal Large Language Models (MLLMs) have achieved breakthrough progress in Document Understanding [29], demonstrating unprecedented capabilities in complex visual layout analysis and cross-modal reasoning. However, as model scale and performance escalate, a critical challenge has emerged: existing Document Visual Question Answering (Doc-VQA) evaluation frameworks focus almost exclusively on final answer accuracy [23, 21, 35, 24, 45, 22], neglecting the logical path through which the model derives that answer—namely, the precise extraction of evidence. Consequently, the true depth and reliability of a model’s comprehension remain largely unverified.

In high-stakes domains such as legal consultation, financial auditing, and evidence-based medicine, "evidence" is the cornerstone of decision-making [15, 47]. An answer-only evaluation masks a critical failure mode: models might rely on pre-trained background knowledge to "make a guess," or land on the correct answer despite grounding it in the wrong passage. Such black-box reasoning poses uncontrollable risks of hallucination [43, 54]. Therefore, an urgent need exists for a benchmark that simultaneously evaluates answer accuracy and evidence faithfulness towards Trustworthy Document Intelligence, bridging the critical gap between text generation and source verification.

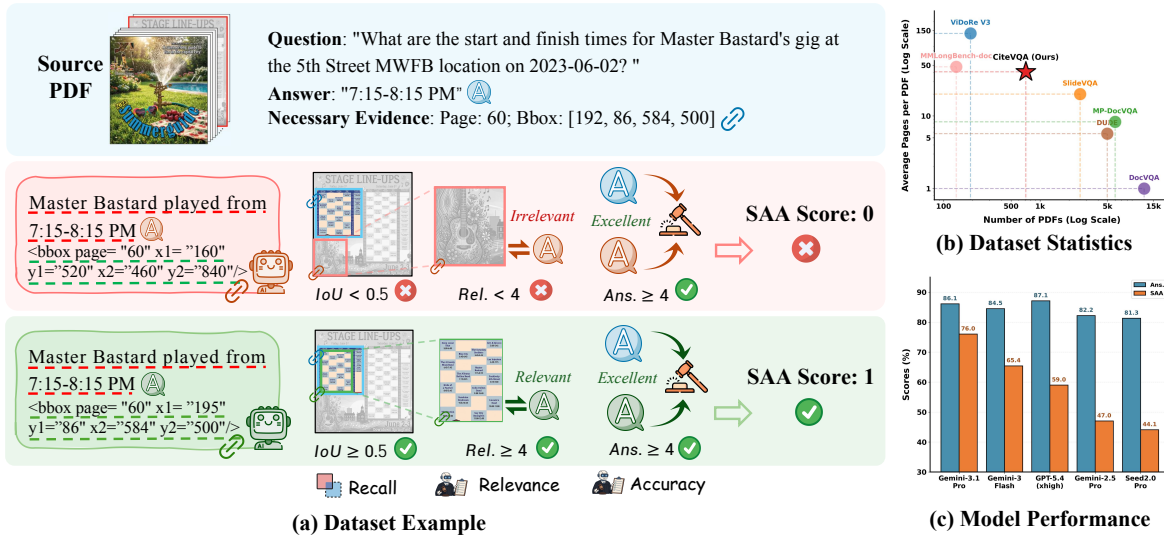


Figure 1: Overview of the CiteVQA benchmark. (a) An example task requiring both correct answers and precise evidence citations to satisfy the Strictly Attributed Accuracy (SAA) metric. (b) Dataset statistics: CiteVQA achieves a balance between document scale and page counts, better reflecting real-world complexity. (c) Performance of MLLMs: Despite high question accuracy, a significant gap exists in SAA due to "Attribution Hallucination".

To address these limitations, we introduce **CiteVQA**: A Benchmark for Faithful Evidence Attribution. Designed for long-form, multi-domain, and cross-lingual scenarios, CiteVQA comprises 1,897 high-quality questions derived from 711 PDFs across seven major domains. As illustrated in Figure 1b, CiteVQA strikes a delicate balance between document quantity and length to better simulate real-world complexity. Unlike traditional tasks, CiteVQA mandates that models provide the precise PDF source supporting their answer at the granularity of *element-level* bounding-box citations, thereby ensuring that every generated claim is visually verifiable by human users.

Constructing such a benchmark is challenging, as manual annotation is prohibitively expensive and prone to inconsistencies [19]. To this end, we developed a highly scalable, automated annotation pipeline. By synergizing advanced document parsing models with powerful MLLMs, this flexible pipeline ensures fine-grained precision and consistency, effectively laying the foundation for large-scale citation data generation while mitigating subjective human biases during the annotation process.

For evaluation, we move beyond answer accuracy and introduce a suite of Traceability Metrics. At its core is Strict Attributed Accuracy (**SAA**), a rigorous audit requiring the model to be correct in both its textual response and its visual evidence attribution. This ensures models are only rewarded when their answers are fundamentally grounded in correct evidence. For further diagnosis, we utilize **Recall** to evaluate evidence coverage and **Relevance** to verify logical alignment.

Extensive experiments on 20 mainstream MLLMs reveal a pervasive and concerning phenomenon: **Attribution Hallucination**. As shown in Figure 1c and Table 3, even top-tier models exhibit "pseudo-faithful" behavior, providing correct textual answers while citing entirely wrong locations. The SAA of state-of-the-art models like Gemini-3.1-Pro-Preview caps at 76.0, while leading open-source MLLMs fail to surpass the 25.0 threshold. This uncovers a severe logical fracture in current systems, further amplifying the risk of untraceable hallucinations, which must be resolved before deploying these models in critical real-world applications.

**Contributions** Our main contributions are threefold:

- **The CiteVQA Benchmark and Traceability Metrics:** We introduce an evaluation framework that transitions Doc-VQA from answer-only scoring to joint evidence-answer verification. Anchored by the Strict Attributed Accuracy (SAA) metric, we establish a rigorous standard for measuring element-level citation fidelity.
- **Scalable High-Fidelity Dataset Construction:** We design an automated data generation pipeline that resolves the cost and consistency bottlenecks of granular visual annotation. This approach enables the scalable creation of a robust, expert-validated dataset comprising 1,897 complex queries across 711 multi-page, multi-domain PDFs.
- **Discovery of the "Attribution Hallucination" Phenomenon:** Through a comprehensive audit of 20 leading MLLMs, we expose a critical vulnerability: models frequently output correct text while grounding it in entirely incorrect visual evidence. By demonstrating that state-of-the-art models cap at 76.0 SAA and leading open-source models fail to reach 25.0, we provide the critical instrumentation to advance trustworthy document intelligence.

## 2 Related Work

### Document Visual Question Answering

Document Visual Question Answering (Doc-VQA) has rapidly evolved from basic visual perception to complex, multi-step reasoning. Early benchmarks (e.g., DocVQA [23], InfoVQA [24], OCR-VQA [26]) primarily targeted single-page comprehension, relying heavily on exact textual answer matching for evaluation. While recent efforts have expanded to handling multi-page and full-document contexts (e.g., MP-DocVQA [39], MMLongBench-Doc [21], SlideVQA [35]), they remain fundamentally answer-centric, with evidence annotations largely restricted to the page level. Emerging datasets integrating bounding box (BBox) annotations [19, 49] struggle with inconsistent granularity and a lack of standardized metrics, precluding rigorous audits of reasoning faithfulness. Furthermore, while domain-specific tasks like ChartQA [22] and Charxiv [45] evaluate targeted elements, they do not reflect the diverse, multi-domain, and layout-heavy challenges of real-world documents. In contrast, CiteVQA introduces a comprehensive cross-page, multi-domain framework grounded in element-level BBox citations. By standardizing evidence granularity and introducing joint evaluation metrics, CiteVQA uniquely measures both answer accuracy and structural traceability in complex real-world scenarios.

Table 1: CiteVQA vs. representative Doc-VQA benchmarks. *Gran.*: evidence granularity (**P** page, **B** bounding box, **E** element-level). *Joint*: answer and citation scored by a single sample-level metric.

Benchmark	#Docs	Avg. Pg.	Gran.	Joint
DocVQA [23]	12,767	1.0	P	×
InfoVQA [24]	5,485	1.0	P	×
MP-DocVQA [39]	6,000	8.3	P	×
MMLongBench-Doc [21]	135	47.5	P	×
SlideVQA [35]	2,619	20.0	B	×
ViDoRe V3 [19]	190	137.0	B	×
<b>CiteVQA (ours)</b>	<b>711</b>	<b>40.6</b>	<b>E</b>	<b>✓</b>

### Evidence-based Reasoning in LLMs

As the issue of hallucination in Large Language Models (LLMs) remain a persistent threat [43, 54, 27, 9, 25], evidence-based reasoning has become paramount, particularly in high-stakes domains such as healthcare and law. Recent works like Med-R<sup>2</sup> [20] and GAPS [4] enforce clinical guideline alignment in medicine, while CitaLaw [51] demands explicit source tracing for legal statutes to bolster judicial authority. Meanwhile, MRAMG-bench [47] focuses on multimodal reasoning by proposing evaluation metrics for interleaved image-text responses to measure a model’s information extraction capabilities in complex contexts. However, these prior works primarily concentrate on text-only reasoning or generic multimodal interactions, leaving evidence-grounded reasoning in visually rich documents largely unexplored. Consequently, evaluating a model’s ability to seamlessly link textual answers to precise visual evidence within long-form

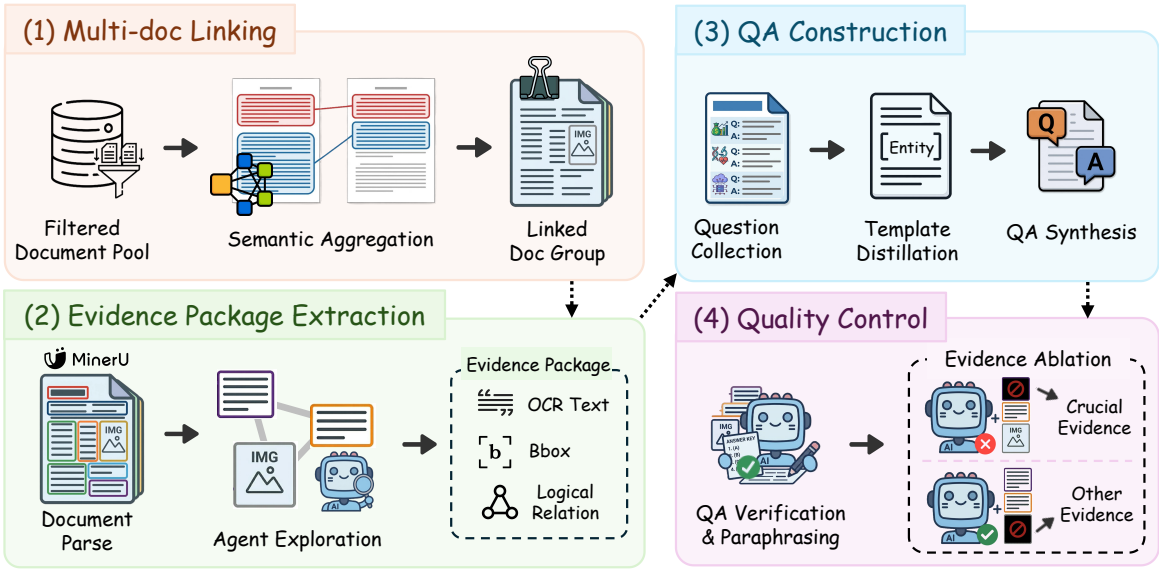


Figure 2: The automated pipeline for CiteVQA. The workflow begins with Multi-doc Linking for semantic document aggregation, followed by Evidence Package Extraction, where intelligent agents navigate and link scattered MinerU parsing results into a cohesive evidence chain. To ensure authenticity, real-world QA pairs are distilled into templates to guide the automated synthesis of rigorous tasks. Finally, the pipeline implements MLLM-based verification and an evidence ablation procedure to precisely identify Crucial Evidence.

documents remains a critical open challenge and largely unexplored.

**Document Intelligence Systems** Early document understanding (or document intelligence) systems predominantly adopted a coarse "page-level retrieval" paradigm. Systems like Colpali [7], VisRAG [48], VDocRAG [36], and M3DocRAG [5] segment documents into page-wise chunks, utilizing multimodal vector search for matching or localization. This macroscopic approach, however, falters on complex queries that demand precise, element-level grounding. Bolstered by the advanced reasoning capabilities of modern MLLMs [56, 53, 16, 11, 10, 30, 46, 41, 6], recent architectures have transcended basic vector matching. SimpleDoc [12] refines precision through an iterative, summary-driven retrieval workflow, while agentic frameworks like DocLens [57], DocDancer [52], and AgenticOCR [44] leverage tool-use to navigate from global pages down to localized visual elements. Yet, despite this systemic evolution toward fine-grained evidence extraction, evaluation paradigms have lagged. Existing benchmarks still primarily focus on end-answer accuracy, completely lacking the rigorous instrumentation needed to verify reasoning paths and visual traceability.

### 3 CiteVQA: A Benchmark for Faithful Evidence Attribution

To construct a high-quality benchmark with fine-grained evidence grounding, we develop an Automated Annotation Pipeline that streamlines the process from raw document parsing to complex question-citation generation. The overall workflow of this pipeline is illustrated in Figure 2. In the following subsections, we first provide a detailed introduction to each stage of the pipeline. Finally, we present a comprehensive analysis of the Data Statistics to highlight the diversity and complexity of the CiteVQA benchmark.

## 3.1 Document Collection

To construct a highly representative and diverse evaluation benchmark, we designed a multi-stage automated filtering pipeline to systematically extract high-quality documents from a vast pool of heterogeneous data. Starting from a corpus of over 100 million raw PDF documents (primarily sourced from Common Crawl<sup>1</sup>; see Appendix A for compliance and ethical standards), we first pre-selected approximately 250k candidate documents through stratified sampling. These candidates then underwent a two-stage MLLM annotation scheme: (1) Coarse-grained stage, identifying the primary domain and language; and (2) Fine-grained stage, performing sub-category classification within each domain.

Ultimately, 711 documents were selected as the source for CiteVQA, achieving a balanced coverage across 7 domains and 30 sub-categories. This fully automated pipeline ensures both reproducibility and scalability.

## 3.2 Question, Answer and Evidence Collection

CiteVQA employs an end-to-end automated construction pipeline. The process first aggregates evidence through multi-document linking, then utilizes high-performance agents to extract complete evidence chains within fine-grained spatial contexts, and finally generates simulated real-world QA pairs through template-driven distillation.

**Multi-Document Linking** To overcome single-document limitations, we propose a linking strategy that aggregates cross-document evidence via semantic alignment. The system identifies candidates through vector similarity and utilizes an LLM to align section-level metadata, integrating isolated documents into logically connected groups  $D$  (retaining single-document form if no associations exist). This provides a robust foundation for complex reasoning across multiple sources; see Appendix B.1 for implementation.

**Evidence Package Extraction** We utilize MinerU2.5 [28, 42] for deep document parsing to obtain fine-grained results containing document IDs, page numbers, bounding box (BBox) coordinates, and OCR content. Drawing inspiration from DocDancer [52] and WebSailor [18], we employ high-performance MLLMs (e.g., Gemini-3.0-Flash-Preview [37]) as intelligent agents. These agents navigate the parsed BBox space to identify and concatenate supporting facts scattered across different pages or documents, ultimately aggregating them into a comprehensive Evidence Package.

**QA Construction** To simulate real-world business scenarios effectively, we collect authentic questions from open-source datasets across various domains (see Appendix B.2) and distill them into a series of templates. During construction, high-performance MLLMs first select the most appropriate logical template based on the characteristics of the Evidence Package, subsequently synthesizing QA pairs automatically based on template constraints and core information within the evidence. This template-guided approach ensures both logical rigor and broad domain coverage.

## 3.3 Quality Control and Assessment

We implement a fully automated verification process to ensure dataset reliability. This includes Answerability Verification to confirm evidence sufficiency, Relevance Filtering to exclude common-knowledge questions, and an ablation-based procedure to identify "Crucial Evidence" for metric validity.

---

<sup>1</sup><https://commoncrawl.org/>

**Answerability Verification and Paraphrasing** To eliminate invalid QA pairs potentially generated during automation, we submit candidate questions along with their dependent evidence screenshots to a powerful MLLM for secondary confirmation. A QA pair is retained only if the model can accurately answer given only the evidence screenshots. Subsequently, the model paraphrases the original template-generated questions to enhance linguistic richness and stylistic diversity while strictly maintaining the original intent.

**Relevance Filtering and Crucial Evidence Identification** To ensure the challenging nature of the dataset, we execute a "zero-document self-test" using Qwen3-VL-235B-A22B-Instruct [2]: questions that the model can answer without any document context (classified as common-knowledge-based) are discarded.

For the core evidence chain determination, we designed an ablation-based crucial evidence identification procedure: each BBox element in the Evidence Package is masked individually before being presented to a powerful MLLM. If the model fails to derive the correct answer after a mask is applied, that element is labeled as "**Crucial Evidence.**" This process ensures the scientific validity of subsequent Recall evaluation metrics.

**Remark** While our pipeline is fully automated to ensure scalability, we conducted human expert evaluation and auxiliary training validation to further guarantee the rigorous quality of the CiteVQA benchmark. Detailed procedures and results of these reliability assessments are provided in Appendix B.3 and B.4.

### 3.4 Dataset Overview and Analysis

As summarized in Table 2 and Figures 3-4, CiteVQA is a diverse benchmark comprising 711 documents across 7 macro-domains, with a realistic average length of 40.6 pages. The 1,897 questions cover varied scenarios including single-doc (52.0%), multi-doc with one gold document (25.7%), and multi-doc with multiple gold documents (22.3%), spanning reasoning types from Complex Synthesis to Multimodal Parsing. Each task requires an average of 2.57 evidence elements, nearly 30% of which are non-textual (tables, images, or equations). Evidence is uniformly distributed across document positions and often spans multiple pages, demanding robust long-context aggregation.

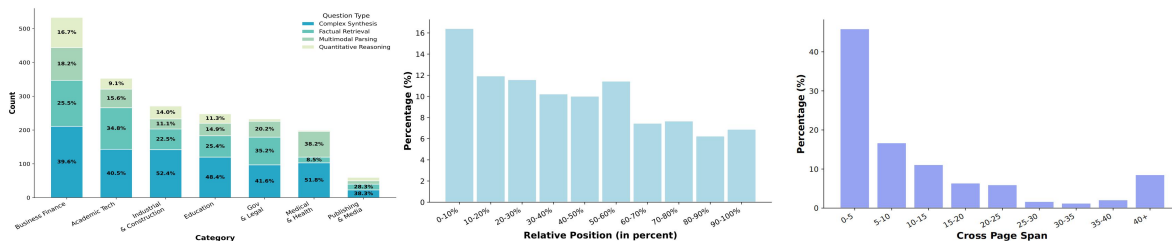


Figure 4: Analysis of question types and evidence distribution in CiteVQA. **Left:** Domain-specific Question Types. **Middle:** Evidence Locality (in relative percent). **Right:** Cross-page Span, quantifying the number of pages spanned by evidences.

## 4 Evaluation

### 4.1 Evaluation Metrics

To evaluate evidence attribution, we introduce a novel set of metrics assessing both answer correctness and trustworthiness in grounding predictions on verifiable evidence.

Table 2: Dataset Statistics

Statistic	Number
<b>Documents</b>	711
- Type (Macro/Micro)	7 / 30
- Avg./Median pages	40.6 / 30.0
- Language (EN/ZH)	451 / 260
<b>Total questions</b>	1,897
- Single-doc	987 (52.0%)
- Multi (1-Gold)	487 (25.7%)
- Multi (N-Gold)	423 (22.3%)
(Question Type)	
- Complex Synthesis	839 (44.23%)
- Factual Retrieval	499 (26.30%)
- Multimodal Parsing	352 (18.56%)
- Quantitative Reasoning	207 (10.91%)
(Evidence Source)	
- Text	2082 (70.12%)
- Table	653 (21.99%)
- Image	209 (7.04%)
- Equation	25 (0.84%)
Avg./Max. question length	137.64 / 500
Avg./Max. answer length	180.48 / 2976
Avg./Max. evidences	2.57 / 10

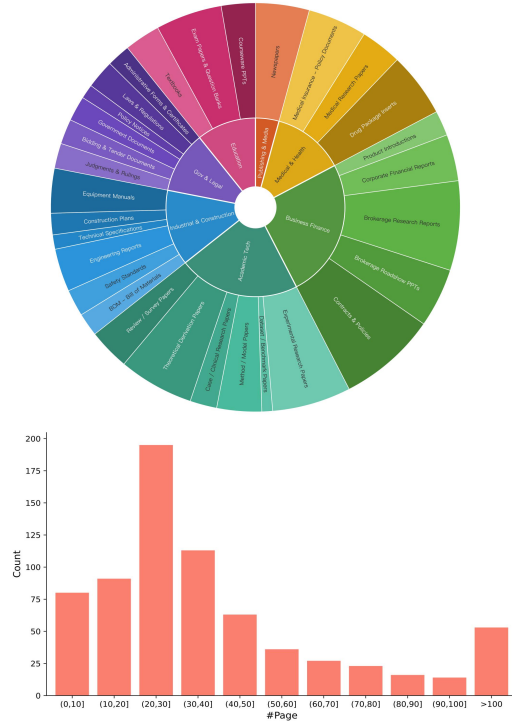


Figure 3: Distribution of documents. **Top:** Document type. **Bottom:** Page Number.

Formally, each sample is represented as  $(D, Q, A_{gt}, \mathcal{B}_{gt})$ , where  $\mathcal{B}_{gt}$  is the set of ground-truth bounding boxes, further categorized into crucial ( $\mathcal{B}_{crucial}$ ) and supplemental ( $\mathcal{B}_{other}$ ) evidence. Each bounding box  $b \in \mathcal{B}$  is defined by  $(doc\_idx, page\_idx, x_1, y_1, x_2, y_2)$ . The model output is  $\hat{Y} = \{(A_1, b_1), \dots, (A_n, b_n)\}$ , where  $\mathcal{B}_{pred} = \{b_1, \dots, b_n\}$  denotes the predicted evidence set.

We define the following key metrics:

**Recall (Rec.)** Measures coarse-grained localization ability, computed at IoU@0.5 between predicted and crucial evidence:

$$Rec. = \frac{1}{|\mathcal{B}_{crucial}|} \sum_{b_{gt} \in \mathcal{B}_{crucial}} \mathbf{1} \left( \max_{b_{pred} \in \mathcal{B}_{pred}} \text{IoU}(b_{pred}, b_{gt}) \geq 0.5 \right)$$

**Relevance (Rel.)** Measures how well each predicted evidence supports its corresponding answer, evaluated by an LLM judge  $\mathcal{J}_{rel}$  on a 0–5 scale:  $Rel. = \frac{1}{n} \sum_{i=1}^n \mathcal{J}_{rel}(A_i, b_i) \in [0, 5]$ .

**Answer Correctness (Ans.)** Measures semantic matching between predicted and ground-truth answers via an LLM judge  $\mathcal{J}_{ans}$ :  $Ans. = \mathcal{J}_{ans}(\{A_1, A_2, \dots, A_n\}, A_{gt}) \in [0, 5]$ .

**Strict Attributed Accuracy (SAA)** A sample-level binary metric requiring both high-quality grounding and answer correctness:  $SAA = \mathbf{1}_{(Ans. \geq 4 \wedge (Rel. \geq 4 \vee Rec. \geq 0.6))}$ .

In addition to the aforementioned metrics, we also evaluate  $Page_{recall}$ , Precision, and F1-score for a more comprehensive assessment of document localization. Owing to space limitations, their formal definitions and detailed evaluation results are deferred to the Appendix C.3 and C.4.

Table 3: **Comprehensive Evaluation of CiteVQA across Different Document Scenarios.** All scores are normalized to a 100-point scale; specifically, Rel. and Ans. scores (originally 0–5) are multiplied by 20 to facilitate direct comparison with Rec. and SAA. For each metric, the best and second-best results are highlighted in **blue** and **green**, respectively.

Model	Single-Doc				Multi (1-Gold)				Multi (N-Gold)				Overall			
	Rec.	Rel.	Ans.	SAA	Rec.	Rel.	Ans.	SAA	Rec.	Rel.	Ans.	SAA	Rec.	Rel.	Ans.	SAA
<i>Closed-source MLLMs</i>																
Gemini-3.1-Pro-Preview	68.9	82.6	86.7	76.0	69.4	84.3	88.0	79.7	55.3	85.3	82.8	71.6	66.0	83.6	86.1	76.0
Gemini-3-Flash-Preview	49.5	76.8	85.3	69.3	42.1	72.3	86.0	61.8	39.5	77.0	81.0	60.5	45.4	75.7	84.5	65.4
Gemini-2.5-Pro	31.5	61.7	83.0	49.4	25.4	58.3	84.1	48.9	20.0	57.3	78.0	39.2	27.4	59.8	82.2	47.0
GPT-5.4	35.9	69.8	87.6	61.7	25.7	62.1	88.3	56.9	25.7	68.2	84.3	55.1	31.0	67.5	87.1	59.0
GPT-5.2	20.9	54.9	71.4	32.6	16.5	63.2	72.4	38.8	13.9	53.0	70.5	30.5	18.2	56.6	71.5	33.7
Qwen3.6-Plus	9.8	26.7	87.1	20.2	5.9	24.6	87.3	18.5	4.6	21.3	81.2	9.8	7.7	25.0	85.9	17.5
Seed2.0-Pro	35.8	60.8	82.9	51.9	18.1	44.9	82.6	33.5	21.5	51.2	76.0	36.2	28.5	54.9	81.3	44.1
GLM-5V-Turbo	18.3	31.2	50.0	14.1	11.7	25.2	44.4	9.8	10.2	28.8	54.3	13.0	14.9	29.2	49.6	12.8
<i>Open-source Large MLLMs</i>																
Kimi-K2.5	8.2	27.7	74.6	21.3	3.5	25.2	74.7	18.9	4.8	26.6	72.9	14.2	6.2	26.8	74.3	19.1
Gemma-4-31B	10.9	31.0	65.7	16.4	14.0	41.0	80.6	29.8	10.4	37.7	67.2	17.8	11.6	35.0	69.8	20.2
Qwen3.5-397B-A17B	6.8	23.6	80.0	17.7	4.0	27.3	71.9	22.2	3.8	23.8	73.5	15.2	5.4	24.6	76.5	18.3
Qwen3.5-122B-A10B	5.9	19.4	78.3	16.0	1.7	20.9	69.0	17.0	1.9	15.6	68.1	9.2	3.9	19.0	73.6	14.8
Qwen3.5-27B	7.0	25.0	79.3	17.1	3.1	28.3	73.1	22.6	3.9	22.6	69.9	11.6	5.3	25.3	75.6	17.3
Qwen3-VL-235B-A22B	15.2	37.8	75.0	25.0	6.2	33.8	68.2	21.6	8.1	31.4	70.9	17.8	11.3	35.3	72.3	22.5
Qwen3-VL-32B	8.0	31.3	75.3	19.3	2.8	29.5	67.6	16.2	7.9	29.8	70.7	14.0	6.6	30.5	72.3	17.3
<i>Open-source Small MLLMs</i>																
Gemma-4-26B-A4B	2.2	15.4	45.6	4.8	4.2	21.4	53.7	9.7	3.5	19.8	48.9	5.5	3.0	17.9	48.4	6.2
Qwen3.5-35B-A3B	2.7	12.6	82.3	9.2	0.5	17.3	73.9	15.6	0.6	12.1	65.5	8.3	1.7	13.7	76.4	10.7
Qwen3.5-9B	2.5	11.7	73.2	8.1	0.3	20.7	58.4	17.7	0.8	14.6	53.5	10.7	1.6	14.7	65.0	11.1
Qwen3-VL-30B-A3B	5.6	15.4	65.4	8.9	0.9	15.9	54.4	8.2	1.7	11.0	63.5	6.4	3.5	14.6	62.2	8.2
Qwen3-VL-8B	1.8	17.6	67.0	8.8	0.0	13.6	53.3	6.8	0.3	9.3	56.4	5.2	1.0	14.7	61.2	7.5

## 4.2 Experimental Setup

We evaluated 20 state-of-the-art MLLMs, encompassing both leading proprietary and open-source models, on the CiteVQA benchmark. For input processing, models received sequential page screenshots via native APIs or OpenAI-compatible interfaces, with image resolutions adapted to their respective context window capacities (see Appendix C.1 for technical specifics). All models were tested using a unified prompt template with a sampling temperature of 1.0. For automated evaluation, we employed Qwen3-VL-235B-A22B as the primary judge (See Analysis of Judges in Appendix C.2).

## 4.3 Main Results

Table 3 presents a comprehensive evaluation of state-of-the-art MLLMs on CiteVQA. Our analysis reveals several critical insights into the current state of faithful evidence attribution.

**The "Attribution Hallucination" Phenomenon** A pervasive gap exists between answer accuracy (Ans.) and Strict Attributed Accuracy (SAA) across all tested models. Notably, while GPT-5.4 and Gemini-3-Flash achieve high answer scores (87.1 and 84.5), their SAA scores drop significantly to 59.0 and 65.4, respectively. This discrepancy confirms an "Attribution Hallucination" effect: while models possess the perceptual capacity to extract information for a correct answer, they lack the ability to precisely link that information to its specific spatial source within the document. This is further

evidenced by low Recall scores; even with a lenient  $\text{IoU} \geq 0.5$  threshold, models frequently fail to localize the crucial evidence or even identify the correct page (See  $\text{Page}_{\text{recall}}$  in Table 12).

**Performance Disparity across Model Tiers** There is a stark performance hierarchy among different model categories. Closed-source MLLMs dominate the benchmark, with Gemini-3.1-Pro-Preview leading at an Overall SAA of 76.0. While GPT-5.4 excels in semantic answer correctness (87.1), it is surpassed by Gemini models in SAA, suggesting Gemini may have more robust native citation-alignment. In contrast, a significant "cliff" exists for Open-source Models, where the strongest (Qwen3-VL-235B) achieves an SAA of only 22.5. Small-scale MLLMs (e.g., Qwen3-VL-8B) struggle the most, with SAA scores often falling below 10.0. This underscores that deploying such small models in high-stakes domains—such as finance, law, or medicine—remains extremely risky, as they lack the fundamental grounding reliability required for professional auditing.

**Impact of Document Scenarios** Task difficulty scales with document complexity. While answer accuracy remains relatively stable across scenarios, attribution becomes markedly harder in multi-document settings. For example, Gemini-3.1-Pro’s Recall drops from 68.9 in Single-Doc tasks to 55.3 in Multi (N-Gold) scenarios. This multi-gold setting consistently yields the lowest SAA scores across the board, highlighting that cross-document evidence linking and complex spatial navigation remain significant frontiers for even the most advanced MLLMs.

## 5 Analysis & Discussion

### 5.1 Fine-grained Results

**Question Type** Results show a significant performance gap between question types (See Figure 5). Models excel in Quantitative Reasoning (e.g., Gemini-3.1-Pro-Preview at 82.6) because numerical computations rely on objective logic and offer clear alignment between evidence and answers. In contrast, the newly introduced Multimodal Parsing task remains a major bottleneck; this category requires models to locate specific document elements based on descriptive cues (such as identifying a particular table by its background color or section header) and subsequently parse the content, leading to substantial difficulties in both precise evidence attribution and final answer generation. See More Fine-grained Results in Appendix C.5

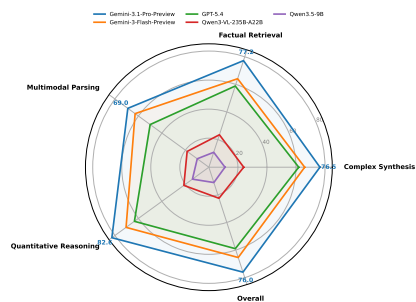


Figure 5: Fine-grained results on various question types (SAA).

### 5.2 Further Analysis of Evidence Attribution

Beyond the initial identification of attribution fallacies, we seek to further explore the nuanced relationship between Attribution and Accuracy.

**Synergy between Attribution and Accuracy** Beyond serving as a metric for trustworthiness, faithful attribution appears to be positively correlated with the model’s reasoning success. As illustrated in Figure 6, after bypassing the "Attribution Hallucination" zone (0-30 points), the Answer Accuracy (Ans.) tends to scale with Evidence Quality ( $\max(\text{Rel.}, \text{Rec.})$ ). This upward trend provides an empirical hint that precise evidence localization might be more than just a post-hoc justification; it potentially acts as a functional foundation that facilitates correct answering in complex document-based tasks.

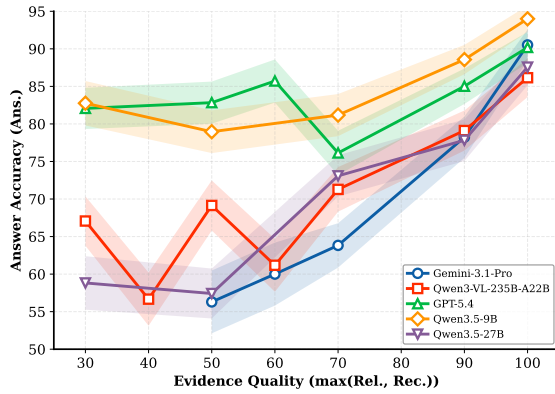


Figure 6: The accuracy of MLLMs exhibits a fluctuating upward trend as evidence quality improves.

**Evidence Attribution as a Potential Performance Driver** To further explore whether enhanced attribution could actively boost performance, we conducted ablation studies by narrowing the candidate search space (Table 4). Restricting the context to GT-Pages consistently yielded gains (up to +5.3%), while providing a single Gold Document in multi-document settings led to substantial leaps, such as +13.4% for Qwen3-VL-8B. These results offer preliminary evidence that some bottleneck in CiteVQA may also lie in the initial "localization" phase. It suggests a promising direction: if models can achieve higher autonomous evidence attribution recall, it might not only enhance transparency but also potentially unlock higher upper bounds for their answering capabilities.

### 5.3 Case Study

To intuitively illustrate the disparity between linguistic performance and attribution accuracy—specifically why some powerful MLLMs achieve high Ans. but low SAA scores—we provide a case study in Figure 7 (see Appendix D for more). For better visualization, cited coordinates are replaced with image crops. While Qwen3-VL-235B-A22B answers correctly (Ans.=1), it yields SAA=0 because its evidence crops are either blank or incomplete. In contrast, Gemini-3.1-Pro-Preview demonstrates faithful grounding; despite a slight offset in the first crop, its second is nearly perfect, resulting in SAA=1. This underscores that a correct answer does not guarantee faithful evidence attribution.

## 6 Conclusion

We introduced CiteVQA, a benchmark designed to advance trustworthy document intelligence by requiring models to provide element-level visual citations alongside answers. Leveraging an automated annotation pipeline, we constructed a large-scale dataset comprising 1,897 questions derived from 711 diverse PDFs. Our systematic audit of top-tier models reveals a critical "Attribution Hallucination" phenomenon, where correct answers are frequently paired with incorrect evidence. By exposing these hidden hallucinations, CiteVQA establishes a rigorous standard for developing interpretable and reliable multimodal systems in high-stakes domains.

Table 4: Ablation studies on Ground Truth (GT) pages and Gold documents. Narrowing the search space consistently leads to performance gains.

Model	Base Setting	GT/Gold Setting
<i>Single-Doc vs. GT Pages</i>		
Qwen3.5-27B	79.3	84.6 (+5.3)
Qwen3-VL-32B	75.3	79.9 (+4.6)
Qwen3.5-9B	73.2	75.2 (+2.0)
Qwen3-VL-8B	67.0	71.1 (+4.1)
<i>Multi (1-Gold) vs. 1 Gold Doc</i>		
Qwen3.5-27B	73.1	81.6 (+8.5)
Qwen3-VL-32B	67.6	72.6 (+5.0)
Qwen3.5-9B	58.4	68.1 (+9.7)
Qwen3-VL-8B	53.3	66.7 (+13.4)

**Question:** What are the specific National Drug Codes for the 10 mL multi-use container of the 40 mg/mL formulation and the 1 mL individual-use unit of the 80 mg/mL strength?

**GT Answer:** The 10 mL multi-dose vial of KENALOG-40 is identified by NDC **0003-0293-28** and the 1 mL single-dose vial of KENALOG-80 by NDC **0003-0315-05**.

---

**Qwen3-VL-235B-A22B Response:**  
 Based on the provided document, the specific National Drug Codes (NDCs) are as follows:  
 \* For the \*\*10 mL multiple-dose vial of the 40 mg/mL formulation\*\*, the NDC is **\*\*0003-0293-28\*\***.  
 \* For the \*\*1 mL single-dose vial of the 80 mg/mL formulation\*\*, the NDC is **\*\*0003-0315-05\*\***: 3-0315-05

**Evaluation:** Rec.=0, Rel.=2, Ans.=5, SAA=0 ❌

---

**Gemini-3.1-Pro-Preview Response:**  
 Based on the provided document, the specific National Drug Codes (NDC) are as follows:  
 - For the 10 mL multiple-dose vial of the 40 mg/mL formulation (KENALOG®-40 Injection), the NDC is **\*\*0003-0293-28\*\***.  
 - For the 1 mL single-dose vial of the 80 mg/mL formulation (KENALOG®-80 Injection), the NDC is **\*\*0003-0315-05\*\***.  
 0 mg/mL, 1 mL single-dose vial NDC 0003-0315-05

**Evaluation:** Rec.=0.5, Rel.=4, Ans.=5, SAA=1 ✅

Figure 7: A Typical Example.

## References

- [1] Josh Achiam, Steven Adler, Sandhini Agarwal, Lama Ahmad, Ilge Akkaya, Florencia Leoni Aleman, Diogo Almeida, Janko Altenschmidt, Sam Altman, Shyamal Anadkat, et al. Gpt-4 technical report. *arXiv preprint arXiv:2303.08774*, 2023.
- [2] Shuai Bai, Yuxuan Cai, Ruizhe Chen, Keqin Chen, Xionghui Chen, Zesen Cheng, Lianghao Deng, Wei Ding, Chang Gao, Chunjiang Ge, et al. Qwen3-vl technical report. *arXiv preprint arXiv:2511.21631*, 2025.
- [3] Tyler Bikaun, Melinda Hodkiewicz, and Wei Liu. Maintnorm: A corpus and benchmark model for lexical normalisation and masking of industrial maintenance short text. In *Proceedings of the Ninth Workshop on Noisy and User-generated Text (W-NUT 2024)*, pages 68–78, 2024.
- [4] Xiuyuan Chen, Tao Sun, Dexin Su, Ailing Yu, Junwei Liu, Zhe Chen, Gangzeng Jin, Xin Wang, Jingnan Liu, Hansong Xiao, et al. Gaps: A clinically grounded, automated benchmark for evaluating ai clinicians. *arXiv preprint arXiv:2510.13734*, 2025.
- [5] Jaemin Cho, Debanjan Mahata, Ozan Irsoy, Yujie He, and Mohit Bansal. M3docrag: Multi-modal retrieval is what you need for multi-page multi-document understanding. *arXiv preprint arXiv:2411.04952*, 2024.
- [6] Chao Deng, Jiale Yuan, Pi Bu, Peijie Wang, Zhong-Zhi Li, Jian Xu, Xiao-Hui Li, Yuan Gao, Jun Song, Bo Zheng, and Cheng-Lin Liu. Longdocurl: a comprehensive multimodal long document benchmark integrating understanding, reasoning, and locating. *arXiv preprint arXiv:2412.18424*, 2024.
- [7] Manuel Faysse, Hugues Sibille, Tony Wu, Bilel Omrani, Gautier Viaud, Céline Hudelot, and Pierre Colombo. Colpali: Efficient document retrieval with vision language models. *arXiv preprint arXiv:2407.01449*, 2024.
- [8] Jessica Foo, Pradyumna Shyama Prasad, and Shaun Khoo. Know or not: a library for evaluating out-of-knowledge base robustness. *arXiv preprint arXiv:2505.13545*, 2025.
- [9] Tianyu Gao, Howard Yen, Jiatong Yu, and Danqi Chen. Enabling large language models to generate text with citations. In *Proceedings of the 2023 Conference on Empirical Methods in Natural Language Processing*, pages 6465–6488, 2023.
- [10] Anwen Hu, Haiyang Xu, Jiabo Ye, Ming Yan, Liang Zhang, Bo Zhang, Chen Li, Ji Zhang, Qin Jin, Fei Huang, and Jingren Zhou. mplug-docowl 1.5: Unified structure learning for ocr-free document understanding. *arXiv preprint arXiv:2403.12895*, 2024.
- [11] Yupan Huang, Tengchao Lv, Lei Cui, Yutong Lu, and Furu Wei. Layoutlmv3: Pre-training for document ai with unified text and image masking. In *Proceedings of the 30th ACM International Conference on Multimedia*, pages 4083–4091, 2022.
- [12] Chelsi Jain, Yiran Wu, Yifan Zeng, Jiale Liu, Shengyu Dai, Zhenwen Shao, Qingyun Wu, and Huazheng Wang. Simpledoc: Multi-modal document understanding with dual-cue page retrieval and iterative refinement. In *Proceedings of the 2025 Conference on Empirical Methods in Natural Language Processing*, pages 28398–28415, 2025.
- [13] Di Jin, Eileen Pan, Nassim Oufattole, Wei-Hung Weng, Hanyi Fang, and Peter Szolovits. What disease does this patient have? a large-scale open domain question answering dataset from medical exams. *arXiv preprint arXiv:2009.13081*, 2020.
- [14] Qiao Jin, Bhuwan Dhingra, Zhengping Liu, William Cohen, and Xinghua Lu. Pubmedqa: A dataset for biomedical research question answering. In *Proceedings of the 2019 conference on empirical methods in natural language processing and the 9th international joint conference on natural language processing (EMNLP-IJCNLP)*, pages 2567–2577, 2019.
- [15] Lu Keer, Zheng Liang, Da Pan, Shusen Zhang, Guosheng Dong, Huang Leng, Bin Cui, Zhonghai Wu, and Wentao Zhang. Med-r2: Crafting trustworthy llm physicians via retrieval and reasoning of evidence-based medicine. In *Proceedings of the ACM Web Conference 2026*, pages 1864–1875, 2026.
- [16] Geewook Kim, Teakgyu Hong, Moonbin Yim, Jeongyeon Nam, Jinyoung Park, Jinyeong Yim, Wonseok Hwang, Sangdoon Yun, Dongyoon Han, and Seunghyun Park. Ocr-free document understanding transformer. In *European Conference on Computer Vision*, pages 498–517. Springer, 2022.

- [17] Hugo Laurençon, Lucile Saulnier, Léo Tronchon, Stas Bekman, Amanpreet Singh, Anton Lozhkov, Thomas Wang, Siddharth Karamcheti, Alexander M. Rush, Douwe Kiela, Matthieu Cord, and Victor Sanh. Obelics: An open web-scale filtered dataset of interleaved image-text documents, 2023.
- [18] Kuan Li, Zhongwang Zhang, Huifeng Yin, Liwen Zhang, Litu Ou, Jialong Wu, Wenbiao Yin, Baixuan Li, Zhengwei Tao, Xinyu Wang, et al. Websailor: Navigating super-human reasoning for web agent. *arXiv preprint arXiv:2507.02592*, 2025.
- [19] António Loison, Quentin Macé, Antoine Edy, Victor Xing, Tom Balough, Gabriel Moreira, Bo Liu, Manuel Faysse, Céline Hudelot, and Gautier Viaud. Vidore v3: A comprehensive evaluation of retrieval augmented generation in complex real-world scenarios. *arXiv preprint arXiv:2601.08620*, 2026.
- [20] Keer Lu, Zheng Liang, Da Pan, Shusen Zhang, Xin Wu, Weipeng Chen, Zenan Zhou, Guosheng Dong, Bin Cui, and Wentao Zhang. Med-r2: Crafting trustworthy llm physicians through retrieval and reasoning of evidence-based medicine. *arXiv e-prints*, pages arXiv-2501, 2025.
- [21] Yubo Ma, Yuhang Zang, Liangyu Chen, Meiqi Chen, Yizhu Jiao, Xinze Li, Xinyuan Lu, Ziyu Liu, Yan Ma, Xiaoyi Dong, et al. Mmlongbench-doc: Benchmarking long-context document understanding with visualizations. *Advances in Neural Information Processing Systems*, 37:95963–96010, 2024.
- [22] Ahmed Masry, Xuan Long Do, Jia Qing Tan, Shafiq Joty, and Enamul Hoque. Chartqa: A benchmark for question answering about charts with visual and logical reasoning. In *Findings of the association for computational linguistics: ACL 2022*, pages 2263–2279, 2022.
- [23] Minesh Mathew, Dimosthenis Karatzas, and CV Jawahar. Docvqa: A dataset for vqa on document images. In *Proceedings of the IEEE/CVF winter conference on applications of computer vision*, pages 2200–2209, 2021.
- [24] Minesh Mathew, Viraj Bagal, Rubèn Tito, Dimosthenis Karatzas, Ernest Valveny, and CV Jawahar. Infographicvqa. In *Proceedings of the IEEE/CVF Winter Conference on Applications of Computer Vision*, pages 1697–1706, 2022.
- [25] Sewon Min, Kalpesh Krishna, Xixi Lyu, Mike Lewis, Wen-tau Yih, Pang Wei Koh, Mohit Iyyer, Luke Zettlemoyer, and Hannaneh Hajishirzi. Factscore: Fine-grained atomic evaluation of factual precision in long form text generation. In *Proceedings of the 2023 Conference on Empirical Methods in Natural Language Processing*, pages 12076–12100, 2023.
- [26] Anand Mishra, Shashank Shekhar, Ajeet Kumar Singh, and Anirban Chakraborty. Ocr-vqa: Visual question answering by reading text in images. In *2019 international conference on document analysis and recognition (ICDAR)*, pages 947–952. IEEE, 2019.
- [27] Reiichiro Nakano, Jacob Hilton, Suchir Balaji, Jeff Wu, Long Ouyang, Christina Kim, Christopher Hesse, Shantanu Jain, Vineet Kosaraju, William Saunders, et al. Webgpt: Browser-assisted question-answering with human feedback. *arXiv preprint arXiv:2112.09332*, 2021.
- [28] Junbo Niu, Zheng Liu, Zhuangcheng Gu, Bin Wang, Linke Ouyang, Zhiyuan Zhao, Tao Chu, Tianyao He, Fan Wu, Qintong Zhang, et al. Mineru2. 5: A decoupled vision-language model for efficient high-resolution document parsing. *arXiv preprint arXiv:2509.22186*, 2025.
- [29] Linke Ouyang, Yuan Qu, Hongbin Zhou, Jiawei Zhu, Rui Zhang, Qunshu Lin, Bin Wang, Zhiyuan Zhao, Man Jiang, Xiaomeng Zhao, et al. Omnidocbench: Benchmarking diverse pdf document parsing with comprehensive annotations. In *Proceedings of the IEEE/CVF Conference on Computer Vision and Pattern Recognition*, pages 24838–24848, 2025.
- [30] Zhiliang Peng, Wenhui Wang, Li Dong, Yaru Hao, Shaohan Huang, Shuming Ma, and Furu Wei. Kosmos-2: Grounding multimodal large language models to the world. *arXiv preprint arXiv:2306.14824*, 2023.
- [31] Shraman Pramanick, Rama Chellappa, and Subhashini Venugopalan. Spiqa: A dataset for multimodal question answering on scientific papers. *Advances in Neural Information Processing Systems*, 37:118807–118833, 2024.
- [32] Colin Raffel, Noam Shazeer, Adam Roberts, Katherine Lee, Sharan Narang, Michael Matena, Yanqi Zhou, Wei Li, and Peter J Liu. Exploring the limits of transfer learning with a unified text-to-text transformer. *Journal of machine learning research*, 21(140):1–67, 2020.

- [33] Christoph Schuhmann, Richard Vencu, Romain Beaumont, Robert Kaczmarczyk, Clayton Mullis, Aarush Katta, Theo Coombes, Jenia Jitsev, and Aran Komatsuzaki. Laion-400m: Open dataset of clip-filtered 400 million image-text pairs. *arXiv preprint arXiv:2111.02114*, 2021.
- [34] Bytedance Seed. Seed1.8 model card: Towards generalized real-world agency, 2026. URL <https://arxiv.org/abs/2603.20633>.
- [35] Ryota Tanaka, Kyosuke Nishida, Kosuke Nishida, Taku Hasegawa, Itsumi Saito, and Kuniko Saito. Slidevqa: A dataset for document visual question answering on multiple images. In *Proceedings of the AAAI Conference on Artificial Intelligence*, volume 37, pages 13636–13645, 2023.
- [36] Ryota Tanaka, Taichi Iki, Taku Hasegawa, Kyosuke Nishida, Kuniko Saito, and Jun Suzuki. Vdocrag: Retrieval-augmented generation over visually-rich documents. In *Proceedings of the Computer Vision and Pattern Recognition Conference*, pages 24827–24837, 2025.
- [37] Gemini Team, Rohan Anil, Sebastian Borgeaud, Jean-Baptiste Alayrac, Jiahui Yu, Radu Soricut, Johan Schalkwyk, Andrew M Dai, Anja Hauth, Katie Millican, et al. Gemini: a family of highly capable multimodal models. *arXiv preprint arXiv:2312.11805*, 2023.
- [38] Gemma Team, Thomas Mesnard, Cassidy Hardin, Robert Dadashi, Surya Bhupatiraju, Shreya Pathak, Laurent Sifre, Morgane Rivière, Mihir Sanjay Kale, Juliette Love, et al. Gemma: Open models based on gemini research and technology. *arXiv preprint arXiv:2403.08295*, 2024.
- [39] Rubèn Tito, Dimosthenis Karatzas, and Ernest Valveny. Hierarchical multimodal transformers for multipage docvqa. *Pattern Recognition*, 144:109834, 2023.
- [40] Michał Turski, Tomasz Stanisławek, Karol Kaczmarek, Paweł Dyda, and Filip Galiński. Ccpdf: Building a high quality corpus for visually rich documents from web crawl data. In *International Conference on Document Analysis and Recognition*, pages 348–365. Springer, 2023.
- [41] Jordy Van Landeghem, Rubèn Tito, Łukasz Borchmann, Michał Pietruszka, Paweł Józia, Rafał Powalski, Dawid Jurkiewicz, Mickaël Coustaty, Bertrand Ackaert, Ernest Valveny, Matthew Blaschko, Sien Moens, and Tomasz Stanisławek. Document understanding dataset and evaluation (dude). In *Proceedings of the IEEE/CVF International Conference on Computer Vision*, pages 19528–19540, 2023.
- [42] Bin Wang, Tianyao He, Linke Ouyang, Fan Wu, Zhiyuan Zhao, Tao Chu, Yuan Qu, Zhenjiang Jin, Weijun Zeng, Ziyang Miao, et al. Mineru2. 5-pro: Pushing the limits of data-centric document parsing at scale. *arXiv preprint arXiv:2604.04771*, 2026.
- [43] Zhengren Wang, Jiayang Yu, Dongsheng Ma, Zhe Chen, Yu Wang, Zhiyu Li, Feiyu Xiong, Yanfeng Wang, Linpeng Tang, Wentao Zhang, et al. Rare: Retrieval-augmented reasoning modeling. *arXiv preprint arXiv:2503.23513*, 2025.
- [44] Zhengren Wang, Dongsheng Ma, Huaping Zhong, Jiayu Li, Wentao Zhang, Bin Wang, and Conghui He. Agentocr: Parsing only what you need for efficient retrieval-augmented generation. *arXiv preprint arXiv:2602.24134*, 2026.
- [45] Zirui Wang, Mengzhou Xia, Luxi He, Howard Chen, Yitao Liu, Richard Zhu, Kaiqu Liang, Xindi Wu, Haotian Liu, Sadhika Malladi, et al. Charxiv: Charting gaps in realistic chart understanding in multimodal llms. *Advances in Neural Information Processing Systems*, 37:113569–113697, 2024.
- [46] Haoxuan You, Haotian Zhang, Zhe Gan, Xianzhi Du, Bowen Zhang, Zirui Wang, Liangliang Cao, Shih-Fu Chang, and Yinfei Yang. Ferret: Refer and ground anything anywhere at any granularity. *arXiv preprint arXiv:2310.07704*, 2023.
- [47] Qinhan Yu, Zhiyou Xiao, Binghui Li, Zhengren Wang, Chong Chen, and Wentao Zhang. Mramg-bench: a comprehensive benchmark for advancing multimodal retrieval-augmented multimodal generation. In *Proceedings of the 48th International ACM SIGIR Conference on Research and Development in Information Retrieval*, pages 3616–3626, 2025.
- [48] Shi Yu, Chaoyue Tang, Bokai Xu, Junbo Cui, Junhao Ran, Yukun Yan, Zhenghao Liu, Shuo Wang, Xu Han, Zhiyuan Liu, et al. Visrag: Vision-based retrieval-augmented generation on multi-modality documents. *arXiv preprint arXiv:2410.10594*, 2024.

- [49] Wenhan Yu, Zhaoxi Zhang, Wang Chen, Guanqiang Qi, Weikang Li, Lei Sha, Deguo Xia, and Jizhou Huang. Sciegqa: A dataset for scientific evidence-grounded question answering and reasoning, 2026. URL <https://arxiv.org/abs/2511.15090>.
- [50] Aohan Zeng, Xin Lv, Zhenyu Hou, Zhengxiao Du, Qinkai Zheng, Bin Chen, Da Yin, Chendi Ge, Chenghua Huang, Chengxing Xie, et al. Glm-5: from vibe coding to agentic engineering. *arXiv preprint arXiv:2602.15763*, 2026.
- [51] Kepu Zhang, Weijie Yu, Sunhao Dai, and Jun Xu. Citalaw: Enhancing llm with citations in legal domain. In *Findings of the Association for Computational Linguistics: ACL 2025*, pages 11183–11196, 2025.
- [52] Qintong Zhang, Xinjie Lv, Jialong Wu, Baixuan Li, Zhengwei Tao, Guochen Yan, Huanyao Zhang, Bin Wang, Jiahao Xu, Haitao Mi, et al. Docdancer: Towards agentic document-grounded information seeking. *arXiv preprint arXiv:2601.05163*, 2026.
- [53] Yi-Fan Zhang, Xingyu Lu, Shukang Yin, Chaoyou Fu, Wei Chen, Xiao Hu, Bin Wen, Kaiyu Jiang, Changyi Liu, Tianke Zhang, et al. Thyme: Think beyond images. *arXiv preprint arXiv:2508.11630*, 2025.
- [54] Penghao Zhao, Hailin Zhang, Qinhan Yu, Zhengren Wang, Yunteng Geng, Fangcheng Fu, Ling Yang, Wentao Zhang, Jie Jiang, and Bin Cui. Retrieval-augmented generation for ai-generated content: A survey. *Data Science and Engineering*, pages 1–29, 2026.
- [55] Suifeng Zhao, Zhuoran Jin, Sujian Li, and Jun Gao. FinRAGBench-V: A benchmark for multimodal RAG with visual citation in the financial domain. In Christos Christodoulopoulos, Tanmoy Chakraborty, Carolyn Rose, and Violet Peng, editors, *Proceedings of the 2025 Conference on Empirical Methods in Natural Language Processing*, pages 4215–4249, Suzhou, China, November 2025. Association for Computational Linguistics. ISBN 979-8-89176-332-6. doi: 10.18653/v1/2025.emnlp-main.211. URL <https://aclanthology.org/2025.emnlp-main.211/>.
- [56] Ziwei Zheng, Michael Yang, Jack Hong, Chenxiao Zhao, Guohai Xu, Le Yang, Chao Shen, and Xing Yu. Deepeyes: Incentivizing "thinking with images" via reinforcement learning. *arXiv preprint arXiv:2505.14362*, 2025.
- [57] Dawei Zhu, Rui Meng, Jiefeng Chen, Sujian Li, Tomas Pfister, and Jinsung Yoon. Doclens: A tool-augmented multi-agent framework for long visual document understanding. *arXiv preprint arXiv:2511.11552*, 2025.
- [58] Wanrong Zhu, Jack Hessel, Anas Awadalla, Samir Yitzhak Gadre, Jesse Dodge, Alex Fang, Youngjae Yu, Ludwig Schmidt, William Yang Wang, and Yejin Choi. Multimodal C4: An open, billion-scale corpus of images interleaved with text. *arXiv preprint arXiv:2304.06939*, 2023.

## Appendix

### A Data Compliance & Ethics Statement

**Data Acquisition from Common Crawl** The 707 PDF documents included in the CiteVQA benchmark are sourced from Common Crawl, a neutral, non-profit public web archive. Our data acquisition process strictly adheres to the Common Crawl Terms of Use<sup>2</sup> and ensures all operations are conducted within the scope permitted by the Robots Exclusion Protocol, demonstrating our utmost respect for the intentions of original content distributors.

**Adherence to Common Standards for Data Distribution** Regarding data derived from Common Crawl, CiteVQA strictly follows the common consensus and academic norms of the multimodal and document intelligence fields. Drawing on the distribution paradigms of landmark works—such as T5 [32], MMC4 [58], OBELICS [17], and CCpdf [40], which focuses specifically on PDF parsing—we have implemented an academically recognized compliance workflow (i.e., distributing only public download links).

We have open-sourced the structured metadata and spatial coordinates (Bounding Boxes) annotated by our automated data pipeline. We ensure that our PDF usage logic remains consistent with large-scale open-source datasets like LAION [33] to promote academic reproducibility while maintaining the compliance of the content distribution chain.

**Copyright Respect and Protection of Rights Holders** All PDF documents in this dataset sourced from Common Crawl are clearly attributed in the repository’s metadata. We hold the legal rights of original copyright holders in the highest regard. If any owner of the relevant documents believes that the indexing or usage within this benchmark is inappropriate, please contact us. We commit to cooperating promptly with the removal or updating of the relevant content upon verification of the rights holder’s identity.

**Vision: Advancing Transparent and Trustworthy AI Auditing** The core vision of CiteVQA is to address the issue of "evidence Attribution Hallucination" in MLLMs when processing complex documents. Inspired by the ethical guidelines of OBELICS [17], we firmly believe that establishing transparent, traceable, and open-source benchmarks is key to building a responsible AI ecosystem. By constructing this evidence-chain benchmark, we aim to provide the community with an auditable and reproducible research tool, pushing global document intelligence research toward a more faithful and transparent future.

---

<sup>2</sup><https://commoncrawl.org/terms-of-use>

## B Details of CiteVQA Pipeline

### B.1 Details of Multi-Document Linking

**Semantic Profiling and Dense Retrieval** To mitigate semantic truncation caused by directly embedding long documents, we first use MLLM to construct a semantic profile for each document  $d_i$ , extracting metadata such as document type, core thesis, and section units. These profiles serve as high-level descriptors that capture the global context of the document beyond simple text snippets. The extracted metadata is then mapped to normalized vectors via an encoder. For an anchor document  $d_a$ , the top- $K_{doc}$  (default 5) candidate documents are selected based on cosine similarity to form the candidate pool  $C_a$ , ensuring that only the most contextually relevant documents are considered for expensive fine-grained analysis.

**Fine-Grained Alignment via LLM** While coarse retrieval identifies document-level relevance, cross-document QA requires precise segment-level evidence chains. We input all section units from both the anchor and candidate documents into an LLM to perform chain-of-thought (CoT) cross-document matching. The model is prompted to reason through the structural hierarchy of each document to find logical bridges between them. The model outputs structured association groups, including the anchor section, candidate section, a similarity score  $s \in [0, 1]$ , and a brief rationale for the connection. We limit the output to a maximum of 5 matching groups with 1–3 related segments per group to maintain high information density. The system retains the best matches in descending order of scores and returns an empty list when no reliable match is found, thereby filtering out noisy or coincidental associations.

**Spatial Mapping and Evidence Synthesis** The matched pages from diverse sources are assembled into a synthetic document, which serves as the workspace for generating complex QA pairs spanning  $\geq 2$  source documents. A critical component of this process is the element-level bijective function  $f_{map}$ , which maintains a persistent link between the synthetic layout and the original files. This function maps the synthetic evidence bounding boxes back to their original spatial coordinates in the source PDF. By ensuring that every byte of synthesized evidence is traceable to its original page, the system fundamentally eliminates visual hallucinations and ensures the absolute fidelity of the citation annotations.

### B.2 Details of Template Distillation

To simulate real-world business scenarios effectively, we collected diverse problems from multi-domain open-source datasets and distilled them into a series of templates.

Table 5 details the distribution of the datasets used in our framework, covering 5 key domains to ensure broad representation. We would like to express our sincere gratitude to the contributors of these open-source projects for their invaluable support to the research community.

Table 5: Distribution of Multi-domain Open-source Datasets

Domain	Dataset	License
Academic Tech	SPIQA [31]	CC BY 4.0
Medical & Health	MedQA [13]	MIT
	PubMedQA [14]	MIT
Business Finance	ViDoRe V3 [19]	CC BY 4.0
Industrial & Construction	MaintNorm [3]	MIT
	ViDoRe V3 [19]	CC BY 4.0
Gov & Legal	PolicyBench [8]	OpenRail

We employed Gemini-3.1-Pro-Preview to extract four core categories of templates from the aforementioned datasets (see Table 6). These templates guide the MLLM to synthesize logically rigorous QA pairs based on specific evidence packages.

Table 6: Classification and Examples of Templates

Category	Template and Representative Example
Factual Retrieval	<b>Template:</b> What is the [Metric] for [Entity]’s [Segment] in [Time Period]? <b>Example:</b> What is the net interest margin for Citigroup’s banking segment in 2024?
Complex Synthesis	<b>Template:</b> Synthesize the [Entity] management’s outlook for [Metric] in [Time Period]. <b>Example:</b> Synthesize the Bank of America management’s outlook for credit loss provisions in 2025.
Quantitative Reasoning	<b>Template:</b> Determine the [Metric] for [Entity] by subtracting [Value A] from [Value B]. <b>Example:</b> Determine the tangible common equity for Citigroup by subtracting goodwill from total equity.
Multimodal Parsing	<b>Template:</b> On which page and in which paragraph is [Visual Style] located? <b>Example:</b> On which page and in which paragraph are the green italic numbers located?

### B.3 Details of Expert Evaluation

Despite the automated production, we invited several PhD-level experts to conduct sampling audits of 200 randomly selected CiteVQA outputs, focusing on question difficulty, answer quality, and the quality of crucial evidence. To ensure consistency in the evaluation standard, the experts followed the same prompt templates as the models, the details of which are provided in Appendix E.1. The audit results (Table 7) confirm the high quality of the automated pipeline, demonstrating appropriate question difficulty and high-quality annotation.

**Remark on Compensation** All human experts involved in data annotation and evaluation (including Appendix B.3 and C.2) were compensated with a task-based honorarium that exceeds the local minimum hourly wage, ensuring fair labor practices.

Table 7: Annotation evaluation results on 200 sampled CiteVQA instances (5-point Likert scale, averaged across human experts).

Judge / Metric	Question Difficulty	Answer Quality	Evidence Quality
Gemini-3-Flash	2.81	4.57	4.93
Qwen3-VL-235B	2.73	4.62	4.89
Human Expert	2.97	4.43	4.91

### B.4 Details of Auxiliary Training Validation

To assist in validating the effectiveness of the automated pipeline in real-world training, we conducted an alignment experiment based on the ViDoRe V3 [19] corpus in Table 8. Following the same PDFs, we generated 3k samples via CiteVQA and compared their performance against the original 5k human-annotated samples in AgenticOCR [44] SFT training. Overall, CiteVQA Pipeline nearly reaches the performance level of human-annotated data.

Table 8: Performance comparison on FinRAGBench-V [55] (subset with bounding boxes) and the held-out test set of ViDoRe V3. **Page<sub>acc</sub>** measures page-level judgment ability; **Recall<sub>min</sub>** indicates coarse-grained localization; **Recall<sub>EM</sub>** reflects exact-grained localization. On FinRAGBench-V, CiteVQA Pipeline (3k) achieves comparable or slightly better performance than Vidore Original (5k). On ViDoRe V3, Vidore Original shows a slight advantage.

Training Data	FinRAGBench-V (subset w. bbox)					ViDoRe V3 (test set)				
	Page <sub>acc</sub>	Recall <sub>min</sub>	Prec <sub>min</sub>	F1 <sub>min</sub>	Recall <sub>EM</sub>	Page <sub>acc</sub>	Recall <sub>min</sub>	Prec <sub>min</sub>	F1 <sub>min</sub>	Recall <sub>EM</sub>
Vidore Original (5k)	97.7	83.0	85.2	82.7	35.4	94.7	83.4	82.2	81.0	48.3
CiteVQA Pipeline (3k)	97.7	82.8	86.0	81.3	40.6	93.5	79.5	82.4	78.8	45.3

In the following, we describe the technical implementation of our distillation strategy, the specific tools provided to the model during training, and the rejection sampling criteria used to ensure the high quality of the resulting trajectories.

**Trajectory Distillation via Rejection Sampling** We follow the same SFT training data distillation pipeline as AgenticOCR [44]. Specifically, we use the CiteVQA pipeline to generate a set of synthetic data from the original PDF files of ViDoRe V3. The data format is similar to that of the original ViDoRe dataset, namely (I, Q, A, E), representing Image, Question, Answer, and Evidence Bbox, respectively.

For both batches of data, we adopt the AgenticOCR approach: we first equip the model with an image\_zoom\_and\_ocr\_tool (allowing the model to zoom into image regions and obtain OCR results), and then perform rejection sampling on the trajectories generated by Gemini-3-Pro-Preview based on an IoU threshold. This yields 3k and 5k high-quality samples, respectively.

**Training Setup** We follow the same training protocol as AgenticOCR: only the tokens generated by the assistant (including reasoning steps and tool calls) contribute to the loss; tokens corresponding to user prompts and tool observations are masked out. The hyperparameters are set as follows: a learning rate of  $1 \times 10^{-5}$ , training for 6 epochs on 8 H200 GPUs.

**Model Evaluation** We evaluate on two test sets. The first is the FinRAGBench-V [55] subset with bounding box annotations (approximately 200 samples). The second is the held-out, manually annotated test set from ViDoRe V3 that is completely disjoint from the training set (approximately 400 samples). The evaluation metrics are identical to those used in AgenticOCR. The final results are reported in Table 8.

## C Details & More Results of Experiments

### C.1 Details of Experimental Setup

**Input Processing Details** For the Gemini series, we utilized the native File API.

For other models, PDF documents were converted to 150 DPI screenshots. To ensure fairness across different context limits:

- **Long-context Models:** Provided with original 150 DPI screenshots.
- **Standard-context Models:** Screenshots were adaptively downscaled according to the specific context constraints of each model family (details provided in Table 9).

Table 9: Model Categorization and Detailed Input Processing Strategies

Category	Models	Resolution and Processing Strategy
<b>Gemini Series [37]</b>	Gemini-3.1-Pro-Preview, Gemini-3-Flash-Preview, Gemini-2.5-Pro	<b>Native File API:</b> Directly processed via the Google Cloud document interface without manual rasterization.
<b>1M Context</b>	GPT-5.4, GPT-5.2 [1], Qwen3.6-Plus	<b>Full Resolution:</b> 150 DPI page screenshots provided as-is to leverage the expansive context window.
<b>256k Context</b>	Qwen3.5 Family, Qwen3VL Family [2], Gemma4 Family [38], Kimi-K2.5 [38], Seed-2.0-Pro [34]	<b>Standard Scaling:</b> Screenshots are adaptively downscaled to a maximum of $1024 \times 1024$ pixels, preserving the original aspect ratio.
<b>200k Context</b>	*Only for GLM-5V-Turbo [50]	<b>Compact Scaling:</b> Screenshots are adaptively downscaled to a maximum of $768 \times 768$ pixels to prevent context overflow while maintaining structural integrity.

Table 10: Impact of input resolution on CiteVQA performance using Qwen3-VL-235B-A22B. We compare our standard scaling ( $1024^2$ ) against reduced pixel budgets to evaluate the sensitivity of evidence attribution to visual clarity. SAA highlights the precipitous drop in grounding reliability as resolution decreases.

Resolution Strategy	Total Pixels	Rec.	Rel.	Ans.	SAA
Full Resolution (Standard)	$1024^2$ ( $1.0\times$ )	11.3	35.3	72.3	22.5
Half-Pixel Scaling	$1024^2/2$ ( $\approx 724^2$ )	4.2	23.6	66.8	11.8
Quarter-Pixel Scaling	$1024^2/4$ ( $512^2$ )	1.6	17.2	53.5	5.3

**Trade-off Analysis of Input Resolution** The results in Table 10 justify our choice of  $1024 \times 1024$  as the standard resolution for evaluation. We observe that while the answer accuracy (Ans.) decreases moderately with lower resolutions, the evidence attribution metrics—particularly Rec. and SAA—exhibit a sharp, non-linear collapse. For instance, halving the total pixels (from  $1024^2$  to  $\approx 724^2$ ) leads to a near-50% reduction in SAA (from 22.5% to 11.8%), indicating that precise localization is highly sensitive to visual fidelity. Although further increasing the resolution might yield marginal gains,  $1024 \times 1024$  represents a critical "saturation point" for most current MLLMs. Exceeding this threshold would surpass the native token limits and internal position embedding constraints of many models (e.g., the Qwen3VL and Gemma families). Thus, our standard scaling maintains an optimal balance between preserving fine-grained document details and adhering to the architectural limits of diverse model families.

**Inference Settings** All experiments were conducted using a unified prompt (See Appendix E.2). The maximum output length was capped at 4,096 tokens to allow for extensive reasoning. For the Qwen3VL family, the "Instruct" versions were consistently used. For the Qwen3.5 series, the Thinking mode was enabled by default. All GPT models were configured with the highest reasoning effort (xhigh), and Gemini models were run with the maximum thinking mode setting.

**Deployment of Open-source Models** We utilized a standardized inference infrastructure consisting of 8xNVIDIA H200 GPUs to ensure consistent latency and sufficient VRAM for high-resolution document processing.

## C.2 Analysis of Different Judges

**Validation of Automated Evaluation via Human Study** To verify the reliability of our automated evaluation pipeline, we conducted a human expert study on 200 randomly selected samples, comparing human scores against those generated by Gemini-3-Flash-Preview and Qwen3-VL-235B-A22B. As detailed in Table 11, we applied the Friedman test—a non-parametric statistical test—to determine if any significant differences existed between the judges. The resulting  $p$ -values for both Rel. and Ans. consistently exceeded the 0.05 threshold (ranging from 0.14 to 0.53) across different inference models. These results indicate that there is no statistically significant deviation between our automated judges and human experts, confirming that the LLM-based scoring system provides a robust and faithful proxy for human judgment in assessing document grounding and response quality.

Table 11: Different Metrics between different judges.  $p$ -values  $> 0.05$  indicate no statistically significant difference between automated LLM judges and human experts across all metrics.

Judge / Infer Model	GPT-5.4		Gemini-3.1-Pro	
	Rel.	Ans.	Rel.	Ans.
Gemini-3-Flash-Preview	2.87	4.51	4.06	4.67
Qwen3-VL-235B-A22B	3.08	4.42	4.12	4.57
Human Expert	2.92	4.44	4.03	4.59
P-value (Friedman Test)	0.16	0.14	0.53	0.21

## C.3 More Evaluation Metrics

To provide a multi-dimensional perspective on document localization and evidence attribution, we introduce several supplementary metrics. These indicators offer a more granular analysis of the model’s performance in identifying relevant document components.

**Page-level Recall (Page. / Page<sub>recall</sub>)** This metric assesses the model’s coarse-grained ability to locate the correct pages containing the necessary evidence. A predicted evidence is considered a "page hit" if its page index matches any page index in the set of crucial evidence.

$$\text{Page.} = \frac{|\{p \in \mathcal{P}_{\text{crucial}} \mid \exists \hat{p} \in \mathcal{P}_{\text{pred}}, \hat{p} = p\}|}{|\mathcal{P}_{\text{crucial}}|}$$

where  $\mathcal{P}_{\text{pred}}$  and  $\mathcal{P}_{\text{crucial}}$  denote the sets of page indices from the predicted and ground-truth crucial evidence, respectively.

**Precision (Prec.)** While Recall focuses on coverage, Precision measures the spatial accuracy of the predicted bounding boxes relative to the entire evidence set  $E$  (including both crucial and auxiliary

evidence). It penalizes the model for generating redundant or irrelevant boxes:

$$\text{Prec} = \frac{1}{|\mathcal{B}_{\text{pred}}|} \sum_{b_{\text{pred}} \in \mathcal{B}_{\text{pred}}} \mathbf{1}_{(\max_{b_{\text{gt}} \in \mathcal{B}_{\text{gt}}} \text{IoU}(b_{\text{pred}}, b_{\text{gt}}) \geq 0.5)}$$

where  $\mathcal{B}_{\text{all}}$  represents the set of all ground-truth bounding boxes associated with the evidence package.

**F1-Score (F1)** To balance the trade-off between localization recall and precision, we report the  $F_1$  score, which is the harmonic mean of the standard Recall (Rec.) defined in the main text and the Precision (Prec.) defined above:

$$F_1 = 2 \cdot \frac{\text{Prec.} \cdot \text{Rec.}}{\text{Prec.} + \text{Rec.}}$$

This metric provides a single scalar value to evaluate the overall efficiency of the evidence extraction process, ensuring the model is both thorough and concise in its attribution.

### C.4 More Results of Experiments

**Widespread Deficiency in Coarse-grained Attribution** A striking observation from Table 12 is that Page-level Recall (Page.) remains remarkably low for the vast majority of models. This indicates that the failure in evidence attribution is not merely a consequence of weak fine-grained grounding (i.e., missing the exact box), but a more fundamental inability to navigate to the correct document page. While the Gemini-3 series demonstrates strong navigation (above 87% Overall Page.), many advanced models like GPT-5.2 (69.3% Overall Page.) and Qwen3-VL-235B-A22B (57.8% Overall Page.) frequently fail to even locate the relevant page. This "coarse-level blindness" suggests that before addressing spatial precision, models must first overcome significant hurdles in document-level retrieval and page indexing.

**Impact of Multi-document Complexity** The challenge of attribution is significantly exacerbated as the environment shifts from Single-Doc to Multi-Doc (N-Gold) settings. In these high-density scenarios, even top-tier models exhibit a sharp performance collapse. For instance, GPT-5.4 sees its Page-level Recall drop from 88.5% in Single-Doc to 75.4% in N-Gold, while its F1-score falls from 29.6% to 20.6%. For many open-source models, the Multi-Doc setting acts as a performance ceiling; for example, Qwen3-VL-235B-A22B experiences a significant decline in Page-level Recall, dropping from 64.4% to 50.5%. This trend underscores that current MLLMs lack the robustness required for multi-document reasoning, a deficit that directly fuels the observed "Attribution Hallucination."

### C.5 More Fine-grained Results

**Document Type** Our cross-domain evaluation reveals that performance varies significantly depending on document structure (See Figure 8): models achieve peak performance in the Academic Tech domain (e.g., Gemini-3.1-Pro-Preview at 85.0) due to the highly standardized layouts and logical rigor of academic papers, which facilitate precise evidence attribution. Conversely, the Publishing & Media domain presents the greatest challenge, with the highest SAA reaching only 63.3, as the complex typographic designs, non-linear content distribution, and intricate image-text interleaving inherent in newspapers and magazines severely hinder models' spatial perception and cross-page reasoning capabilities.

Table 12: Detailed attribution performance of MLLMs across different document scenarios. Page. denotes Page-level Recall; Rec., Prec., and F1 represent bounding-box-level Recall, Precision, and F1-score respectively. For each metric, the best and second-best results are highlighted in **blue** and **green**, respectively.

Model	Single-Doc				Multi (1-Gold)				Multi (N-Gold)				Overall			
	Page.	Rec.	Prec.	F1	Page.	Rec.	Prec.	F1	Page.	Rec.	Prec.	F1	Page.	Rec.	Prec.	F1
<i>Closed-source MLLMs</i>																
Gemini-3.1-Pro-Preview	88.8	<b>68.9</b>	<b>63.1</b>	<b>62.0</b>	91.5	<b>69.4</b>	<b>62.8</b>	<b>61.6</b>	81.4	<b>55.3</b>	<b>49.4</b>	<b>48.6</b>	87.9	<b>66.0</b>	<b>59.9</b>	<b>58.9</b>
Gemini-3-Flash-Preview	<b>92.8</b>	<b>49.5</b>	<b>37.0</b>	<b>37.9</b>	<b>94.3</b>	<b>42.1</b>	<b>30.1</b>	<b>31.3</b>	<b>86.5</b>	<b>39.5</b>	<b>29.9</b>	<b>30.3</b>	<b>91.8</b>	<b>45.4</b>	<b>33.7</b>	<b>34.5</b>
Gemini-2.5-Pro	<b>92.3</b>	31.5	24.8	24.6	<b>93.5</b>	25.4	18.3	18.6	<b>81.7</b>	20.0	17.4	16.2	<b>90.3</b>	27.4	21.5	21.2
GPT-5.4	88.5	35.9	29.6	29.6	79.9	25.7	22.4	20.9	75.4	25.7	21.2	20.6	<b>83.4</b>	<b>31.0</b>	25.9	25.4
GPT-5.2	67.4	20.9	20.4	18.6	75.9	16.5	15.4	14.8	66.1	13.9	13.4	12.0	<b>69.3</b>	<b>18.2</b>	<b>17.6</b>	<b>16.2</b>
Qwen3.6-Plus	50.0	9.8	9.7	8.7	51.7	5.9	6.0	5.5	47.5	4.6	4.9	4.3	<b>49.9</b>	<b>7.7</b>	<b>7.7</b>	<b>6.9</b>
Seed2.0-Pro	69.7	35.8	31.8	31.2	59.5	18.1	16.9	15.5	56.4	21.5	18.7	17.2	<b>64.4</b>	<b>28.5</b>	<b>25.4</b>	<b>24.4</b>
GLM-5V-Turbo	48.9	18.3	18.5	16.4	43.3	11.7	12.4	10.8	44.0	10.2	9.3	9.0	<b>46.5</b>	<b>14.9</b>	<b>15.0</b>	<b>13.4</b>
<i>Open-source Large MLLMs</i>																
Kimi-K2.5	44.8	8.2	8.0	7.4	42.4	3.5	3.2	3.0	46.0	4.8	5.7	4.4	<b>44.4</b>	<b>6.2</b>	<b>6.3</b>	<b>5.6</b>
Gemma-4-31B	44.8	10.9	9.8	9.0	56.0	14.0	12.4	11.0	51.1	10.4	11.0	9.0	<b>49.1</b>	<b>11.6</b>	<b>10.7</b>	<b>9.5</b>
Qwen3.5-397B-A17B	48.8	6.8	6.9	6.1	41.6	4.0	3.3	3.4	41.7	3.8	4.5	3.6	<b>45.3</b>	<b>5.4</b>	<b>5.4</b>	<b>4.9</b>
Qwen3.5-122B-A10B	41.5	5.9	5.4	5.2	28.6	1.7	1.7	1.6	30.1	1.9	2.1	1.6	<b>35.6</b>	<b>3.9</b>	<b>3.7</b>	<b>3.5</b>
Qwen3.5-27B	50.2	7.0	6.9	6.0	43.4	3.1	2.4	2.3	45.1	3.9	3.7	3.5	<b>47.3</b>	<b>5.3</b>	<b>5.0</b>	<b>4.5</b>
Qwen3-VL-235B-A22B	64.4	15.2	14.9	13.5	50.7	6.2	5.7	5.4	50.5	8.1	7.5	7.0	<b>57.8</b>	<b>11.3</b>	<b>10.9</b>	<b>10.0</b>
Qwen3-VL-32B	69.0	8.0	7.5	6.8	50.7	2.8	2.7	2.4	52.9	7.9	7.5	7.0	<b>60.7</b>	<b>6.6</b>	<b>6.3</b>	<b>5.7</b>
<i>Open-source Small MLLMs</i>																
Gemma-4-26B-A4B	20.8	2.2	2.7	1.9	22.0	4.2	5.2	3.7	27.5	3.5	3.9	3.2	<b>22.6</b>	<b>3.0</b>	<b>3.6</b>	<b>2.7</b>
Qwen3.5-35B-A3B	35.1	2.7	2.4	2.3	12.4	0.5	0.5	0.5	18.5	0.6	1.0	0.6	<b>25.5</b>	<b>1.7</b>	<b>1.6</b>	<b>1.5</b>
Qwen3.5-9B	33.6	2.5	2.4	2.3	6.2	0.3	0.3	0.3	12.2	0.8	1.3	0.9	<b>21.8</b>	<b>1.6</b>	<b>1.6</b>	<b>1.5</b>
Qwen3-VL-30B-A3B	23.0	5.6	6.1	5.0	7.1	0.9	0.9	0.9	14.1	1.7	2.4	1.6	<b>16.9</b>	<b>3.5</b>	<b>4.0</b>	<b>3.2</b>
Qwen3-VL-8B	43.2	1.8	1.5	1.4	18.9	0.0	0.0	0.0	16.9	0.3	0.2	0.3	<b>31.1</b>	<b>1.0</b>	<b>0.9</b>	<b>0.8</b>

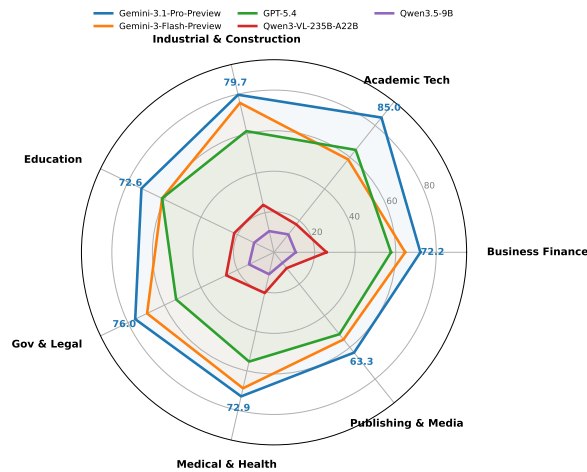


Figure 8: Fine-grained results on various document types (SAA Score).

## D Case Study

**Question:** Assuming we move forward with every single one-year extension permitted by our agreement, what would be the billable amount per hour for both the Technical Lead and the Programmer for each of those supplemental periods?

**GT Answer:** The contract may be renewed for up to five additional one-year periods. For these optional years, the hourly rates for the Technical Lead are \$170 in Year 1, \$176 in Year 2, \$182 in Year 3, \$188 in Year 4, and \$194 in Year 5. For the Programmer role, the hourly rates are \$147 in Year 1, \$152 in Year 2, \$157 in Year 3, \$162 in Year 4, and \$167 in Year 5.

**Crucial Evidence:**

Resource	Contract Optional Years				
	Year 1	Year 2	Year 3	Year 4	Year 5
Technical Lead (hourly rate)	170	176	182	188	194
Programmer (hourly rate)	147	152	157	162	167
SPOC (hourly rate)	298	307	317	327	337

### Gemini-3.1-Pro-Preview Response:

According to the contract, the agreement permits up to 5 additional one-year renewal periods:

This Contract may be renewed in writing by mutual agreement of the parties not less than 30 days before its expiration. The Contract may be renewed for up to 5 additional 1 year periods.

Based on the "Contract Optional Years" pricing table in Appendix A, if all 5 extension years are utilized, the hourly billable rates for those supplemental periods would be:

Resource	Contract Optional Years				
	Year 1	Year 2	Year 3	Year 4	Year 5
Technical Lead (hourly rate)	170	176	182	188	194
Programmer (hourly rate)	147	152	157	162	167
SPOC (hourly rate)	298	307	317	327	337

\*\*Technical Lead (hourly rate):\*\*\n\* \*\*Year 1:\*\* \$170\n\* \*\*Year 2:\*\* \$176\n\* \*\*Year 3:\*\* \$182\n\* \*\*Year 4:\*\* \$188\n\* \*\*Year 5:\*\* \$194\n\*\*Programmer (hourly rate):\*\*\n\* \*\*Year 1:\*\* \$147\n\* \*\*Year 2:\*\* \$152\n\* \*\*Year 3:\*\* \$157\n\* \*\*Year 4:\*\* \$162\n\* \*\*Year 5:\*\* \$167"

Evaluation: Rec.=1, Rel.=5, Ans.=5, SAA=1

### GPT-5.4(-xhigh) Response:

If all five one-year renewal periods permitted under the agreement are exercised, the hourly billing rates are as follows. The agreement specifies that it may be renewed for "up to 5 additional one-year terms."

2.002 Options to Renew  
This Contract may be renewed in writing by mutual agreement of the parties not less than 30 d

The "Contract Optional Years" table in Appendix A lists the hourly rates for these renewal years.

Resource	Contract Optional Years				
	Year 1	Year 2	Year 3	Year 4	Year 5
Technical Lead (hourly rate)	145	150	155	160	165
Programmer (hourly rate)	125	129	133	137	142
SPOC (hourly rate)	255	263	271	280	289

Renewal Period	Technical Lead	Programmer
1st One-Year Renewal	\$170/hour	\$147/hour
2nd One-Year Renewal	\$176/hour	\$152/hour
3rd One-Year Renewal	\$182/hour	\$157/hour
4th One-Year Renewal	\$188/hour	\$162/hour
5th One-Year Renewal	\$194/hour	\$167/hour

Evaluation: Rec.=0, Rel.=1, Ans.=5, SAA=0

Figure 9: Case Study 1. While both models generate correct answers (Ans.=5), Gemini-3.1-Pro-Preview accurately cites the "Contract Optional Years" table (SAA=1). Conversely, GPT-5.4 exhibits "Attribution Hallucination" by providing the correct text but citing an incorrect pricing table (e.g., \$145 vs. \$170 for Year 1), resulting in Rec.=0 and SAA=0.

**Question:** By how much does the electronic energy gap of NbO<sub>2</sub> widen as it transitions from a bond alternation level of 17.1% to its completely dimerized insulating form?

**GT Answer:** 0.26 eV

**Crucial Evidence:**

The occupied split-off flat bands can also exist in nonmetallic of electron transition metal oxides such as the tetragonal compound NbO<sub>2</sub>. This compound shows a metal-insulator transition with an embedded Peierls instability [52], where the Nb-Nb dimerization of structural symmetry breaking determines the electronic structures. Without Nb-Nb dimerization, as shown in Fig. 4(a), there is an internal energy gap, and the Fermi level resides in the principal CB, which makes the system an electron metal. The space group is P4<sub>1</sub> (rutile structure) for this rutile phase. With Nb-Nb dimerization, as shown in Fig. 5(a), the Fermi level is shifted down, entering the internal energy gap, creating occupied split-off flat bands, and opening a band gap of 0.14 eV. The space group is I4<sub>1</sub> for this body-centered insulating phase. The band energy will be lowered by 64 meV/a.u. after symmetry breaking. The band edges change from  $\gamma_1$ ,  $\gamma'_2$  to  $\gamma_1$ ,  $\gamma'_1$  during this C2 process, reflecting that  $d$ -like resonance states within the principal CB shift into the internal energy gap, as also shown in the PDOS of Fig. 4(b). The split-off flat bands will trap one Nb- $d$  electron per formula unit in the Nb-Nb dimer, as shown in Fig. 5(a). (See the Supplemental Material [54] for the occupied split-off flat bands trapping electrons [54].)

where  $d_{long}$  and  $d_{short}$  are the long and short Nb-Nb bonding lengths, respectively. The snapshots of crystallographic structures at different DBAs are generated by linear interpolation between the initial symmetry-unbroken phase (DBA = 0%) and the final symmetry-broken phase (DBA = 20.3%), which are related by DFT calculations with the electronic structures shown in Fig. 8. We pick up four representative snapshots of density of states (DOS) for NbO<sub>2</sub> in Figs. 8(a-d) to show the evolution of occupied split-off flat bands. The Nb- $d$  resonator states reside within the broad principal CB at DBA = 0% [Fig. 8(a)], gradually shift down, still connecting the principal CB at DBA = 15.0% [Fig. 8(b)], enter the internal energy gap, becoming occupied split-off flat bands, producing a band gap of 0.14 eV at DBA = 17.1% [Fig. 8(c)], and further move away from the principal CB with a larger band gap of 0.34 eV at DBA = 20.3% [Fig. 8(d)]. We can see in Fig. 8(c) the whole C2 process with the band gap as a function of DBA. The band gap remains closed with increasing perturbations of DBA, starts to appear until exceeding natural structural perturbations of DBA = 15.1%, and then grows as a linear function of DBA. Note that we do not use the effective  $d$  for calculations of commensurate NbO<sub>2</sub>. This continuous C2 process is also associated with

**Gemini-2.5-Pro Response:**

According to the document, the electronic energy gap of NbO<sub>2</sub> at a bond alternation (DBA) level of 17.1% is 0.14 eV.

The completely dimerized insulating form of NbO<sub>2</sub> has a band gap of 0.40 eV.

Therefore, the widening of the electronic energy gap is the difference between these two values:  
0.40 eV - 0.14 eV = 0.26 eV.

symmetry-broken phase (DBA = 21.3%), which is confirmed by DFT calculations with the electronic structures in Fig. 8. We pick up four representative snapshots of density of states (DOS) for NbO<sub>2</sub> in Figs. 8(a-d) to show the evolution of occupied split-off flat bands. The Nb- $d$  resonator states reside within the broad principal CB at DBA = 0% [Fig. 8(a)], gradually shift down, still connecting the principal CB at DBA = 15.0% [Fig. 8(b)], enter the internal energy gap, becoming occupied split-off flat bands, producing a band gap of 0.14 eV at DBA = 17.1% [Fig. 8(c)], and further move away from the principal CB with a larger band gap of 0.34 eV at DBA = 20.3% [Fig. 8(d)]. We can see in Fig. 8(c) the whole C2 process with the band gap as a function of DBA. The band gap remains closed with increasing perturbations of DBA, starts to appear until exceeding natural structural perturbations of DBA = 15.1%, and then grows as a linear function of DBA. Note that we do not use the effective  $d$  for calculations of commensurate NbO<sub>2</sub>. This continuous C2 process is also associated with

compound NbO<sub>2</sub>. This compound shows a transition with an embedded Peierls instability. Nb-Nb dimerization of structural symmetry determines the electronic structures. Without Nb-Nb dimerization, as shown in Fig. 4(a), there is an internal energy gap, and the Fermi level resides in the principal CB, which makes the system an electron metal. The space group is P4<sub>1</sub> for this body-centered insulating phase. With dimerization, as shown in Fig. 5(a), the Fermi level is shifted down, entering the internal energy gap, creating occupied split-off flat bands, and opening a band gap of 0.14 eV. The space group is I4<sub>1</sub> for this body-centered insulating phase. The band energy will be lowered by 64 meV/a.u. after symmetry breaking. The band edges change from  $\gamma_1$ ,  $\gamma'_2$  to  $\gamma_1$ ,  $\gamma'_1$  during this C2 process, reflecting that  $d$ -like resonance states within the principal CB shift into the internal energy gap, as also shown in the PDOS of Fig. 4(b). The split-off flat bands will trap one Nb- $d$  electron per formula unit in the Nb-Nb dimer, as shown in Fig. 5(a). (See the Supplemental Material [54] for the occupied split-off flat bands trapping electrons [54].)

**Evaluation:** Rec.=0.5, Rel.=4, Ans.=5, SAA=1 ✓

**Qwen3-VL-8B Response:**

The electronic energy gap of NbO<sub>2</sub> widens by 0.2 eV as it transitions from a bond alternation level of 17.1% to its completely dimerized insulating form. This is determined by analyzing Figure 8 on page 14, which shows the evolution of the electronic structure of NbO<sub>2</sub> with increasing bond alternation (DBA). The figure includes a plot of the band gap as a function of DBA. At DBA = 17.1% (Figure 8c), the band gap is 0.34 eV. At the completely dimerized state, which corresponds to DBA = 20.3% (Figure 8d), the band gap is 0.54 eV. The difference is 0.54 eV - 0.34 eV = 0.20 eV.



**Evaluation:** Rec.=0, Rel.=1, Ans.=1, SAA=0 ✗

Figure 10: Case Study 2. While Gemini-2.5-Pro correctly calculates the widening gap (0.40 – 0.14 = 0.26 eV) and cites the corresponding evidence segments (SAA=1), Qwen3-VL-8B fails both semantically and visually. It extracts incorrect values (0.34 and 0.54 eV) from the text and provides irrelevant citations, resulting in Ans.=1 and SAA=0. This case demonstrates that even when evidence is explicitly stated in the text, weaker models struggle with both the retrieval and the logic required for multi-step attribution.

## E Prompt Templates

### E.1 Prompts for CiteVQA Pipeline

#### Prompt for Extracting Evidence Package from PDFs

```

**Role**: Parse a PDF document containing outline, OCR text blocks, bounding boxes, and page screenshots.

**Goal**: Collect high-quality, verifiable evidence bundles to support Q&A, analysis, calculation, and visual extraction.

**Each evidence bundle MUST satisfy**:

1. **Multi-page**: At least 2 different pages.
2. **Multi-element**: At least 2 element types (e.g., text, table, figure, layout).
3. **Complete context**:
   - If including a table/figure, MUST also extract its title, caption, legend, axis labels, footnotes, etc.
   - If an element spans multiple pages (e.g., continued table), MUST extract the complete structure from ALL involved pages (e.g., headers from previous page).

**What to capture**:
- **Text**: Key phrases, definitions, scope notes.
- **Figures**: Captions, axis/legend text, panel labels.
- **Tables**: Full headers, target cells, footnotes.
- **Layout**: Relative position, grouping, visual prominence (e.g., full-width table, top large figure).

**Exploration steps**:
1. Search keywords: "Figure", "Table", "Note", "unit", etc.
2. Extract the hit AND all surrounding relevant elements (enforce complete context for tables/figures).
3. Cross-page link: Connect same metric/entity across different pages.
4. Use screenshots and bounding boxes to confirm type and layout.

**Avoid**:
- Single-element bundles, ID/page-number dependencies, fragmented tables/figures, broad summaries without clear Q&A target.

**Output format**: Return a list of evidence bundles. Generate at least **10** bundles.

```json
[
  {
    "Evidence_package_description": "Brief description of purpose and reasoning value",
    "Evidence_list": [
      {
        "type": "element_type",
        "content": "OCR text content",
        "bbox": [y1, x1, y2, x2],
        "angle": 0,
        "page_id": page_number,
        "element_idx": "element_index"
      }
    ]
  }
]
// At least 5 relevant elements

```

```
]
}]
---
```

### Prompt for Getting Templates from Open-source Datasets

Given question samples, generate one reusable template for each sample.

Return strict JSON only:

```
{
  "samples": [
    {
      "sample_id": 0,
      "category": "...",
      "template_en": "...",
      "template_cn": "...",
      "example_en": "...",
      "example_cn": "..."
    }
  ]
}
```

Requirements:

1. category: "Complex Synthesis", "Factual Retrieval", "Multimodal Parsing", "Quantitative Reasoning",.
2. template\_en/template\_cn must be abstract reusable templates, use placeholders like [Entity], [Date], [Metric], [Section], [Method].
3. example\_en/example\_cn should be one short concrete question in that sample style.
4. Keep semantic consistency within each sample.
5. Must return one item for every sample\_id provided.

### Prompt for Annotation Evaluation

You are an expert evaluator for a VQA benchmark. Your task is to assess the quality of a given QA pair along three dimensions: **Question Difficulty**, **Answer Quality**, and **Crucial Evidence Quality**.

Please follow the scoring criteria below. All scores range from **0** to **5**, where **0** indicates complete failure or unusable quality.

---

**1. Question Difficulty (0-5)**

- **0**: Nonsensical, unanswerable, or no meaningful question.
- **1 to 2 (Simple)**: Direct fact retrieval, minimal reasoning, no cross-document or cross-page synthesis.
- **3 (Moderate)**: Requires basic inference or aggregation from a single document section.
- **4 to 5 (Complex)**: Involves multi-step reasoning, cross-document comparison, contradiction resolution, or indirect evidence extraction.

---

**\*\*2. Answer Quality (0-5)\*\***

- **\*\*0\*\***: No answer or completely irrelevant.
- **\*\*1 to 2 (Poor)\*\***: Largely incorrect, missing key information, or no citation.
- **\*\*3 (Acceptable)\*\***: Correct but overly brief, lacks sufficient justification or citation.
- **\*\*4 to 5 (Good/Excellent)\*\***: Accurate, well-structured, properly cited, and fully addresses the question.

---

**\*\*3. Crucial Evidence Quality (0-5)\*\***

- **\*\*0\*\***: No evidence provided, or evidence completely unrelated.
- **\*\*1 to 2 (Weak)\*\***: Evidence is minimally relevant or insufficient to support the answer.
- **\*\*3 (Moderate)\*\***: Evidence is relevant but incomplete, not optimally cited, or overly redundant.
- **\*\*4 to 5 (Strong)\*\***: Evidence precisely supports the answer, comes from authoritative sections (e.g., tables, core arguments), and includes necessary span-level references.

---

**\*\*Output Format:\*\***

Please output in the following structured format:

---

Question Difficulty: [0 to 5]  
Brief Justification: ...

Answer Quality: [0 to 5]  
Brief Justification: ...

Evidence Quality: [0 to 5]  
Brief Justification: ...

---

## E.2 Prompts for CiteVQA Evaluation

### Prompt for Inference in Single-Doc

# Document Analysis Assistant

Answer the question based on the provided PDF page images, and cite the evidence regions in your answer.

## Evidence Citation Rules

1. Evidence must be at the **element level**: a complete paragraph, a complete table, a complete image, or a complete note. Do not select partial text from a paragraph or a single row from a table, and do not select an entire page or spanning multiple tables/paragraphs. Note: This is very important and will directly affect your score.
2. For **tables and images**, if there are captions or footnotes, they need to be annotated as **separate evidence** with their own bbox, not merged into the table/image bbox.
3. Each piece of cited evidence text should be followed by a `<bbox />` tag indicating the evidence location.
4. When an inference step relies on multiple pieces of evidence, use multiple `<bbox />` tags separately.
5. Pure reasoning/calculation steps do not need `<bbox />`.

## Annotation Format

---

```
<bbox page="page_number" x1="left" y1="top" x2="right" y2="bottom" />
```

---

Page numbers start from 1 (note: ignore original page numbers); coordinates are relative coordinates on the page image, range 0-1000.

## Examples

**Question:** What is the net change in the company's precision copper tube production capacity from 2021 to 2024?

**Answer:**

According to the main text, the company's precision copper tube production capacity increased from 798,000 tons in 2021 to 1.31 million tons in 2024:

```
<bbox page="1" x1="536" y1="65" x2="642" y2="656" />
```

Therefore, the net change = 1.31 - 0.798 = 0.512 million tons.

Additionally, according to "Table 1: Production line renovation will reduce the company's costs", the per-ton comprehensive cost is expected to decrease by 700 yuan/ton after the production line renovation:

```
<bbox page="8" x1="584" y1="65" x2="598" y2="371" />
```

```
<bbox page="8" x1="598" y1="59" x2="712" y2="670" />
```

## Final Reminder

Evidence must be a complete paragraph, a complete table, a complete image, or a complete note. Do not select partial rows from a paragraph or a single row from a table, and do not select an entire page or spanning multiple tables/paragraphs. Note: This is very

important and will directly affect your score.

### Prompt for Inference in Multi-Doc

# Multi-Document Analysis Assistant

Answer the question based on the provided PDF documents, and cite the evidence regions in your answer.

## Document Numbering Rules

- Document numbering starts from 1, corresponding to the order in the `PDF\_Source` list
- Must use the correct document numbers when citing evidence

## Evidence Citation Rules

1. Evidence must be at the **element level**: a complete paragraph, a complete table, a complete image, or a complete note. Do not select partial text from a paragraph or a single row from a table, and do not select an entire page or spanning multiple tables/paragraphs. Note: This is very important and will directly affect your score.
2. For **tables and images**, if there are captions or footnotes, they need to be annotated as **separate evidence** with their own bbox, not merged into the table/image bbox.
3. Each piece of cited evidence text should be followed by a `**bbox` />` tag indicating the evidence location.**
4. When an inference step relies on multiple pieces of evidence, use multiple `**bbox` />` tags separately.**
5. Pure reasoning/calculation steps do not need `**bbox` />`.**

## Annotation Format

---

```
<bbox doc="document_number" page="page_number" x1="left" y1="top" x2="right" y2="bottom" />
```

---

- `doc`: Document number, starting from 1 (corresponding to `PDF\_Source` list order)
- `page`: Page number starting from 1 (note: ignore original page numbers)
- Coordinates are relative coordinates on the page image, range 0-1000

## Examples

**Question:** Compare the revenue data differences between Company in Document 1 and Document 2.

**Answer:**

According to the main text of Document 1, the company's 2023 revenue was 10 billion yuan:

```
<bbox doc="1" page="1" x1="536" y1="65" x2="642" y2="656" />
```

According to the financial report in Document 2, the company's 2023 revenue was 12 billion yuan:

```
<bbox doc="2" page="3" x1="584" y1="65" x2="598" y2="371" />
```

Therefore, the revenue difference reported in the two documents is 2 billion yuan.

## Final Reminder

Evidence must be a complete paragraph, a complete table, a complete image, or a complete note. Do not select partial rows from a paragraph or a single row from a table, and do not select an entire page or spanning multiple tables/paragraphs. Note: This is very

important and will directly affect your score.

### Prompt for Evaluating Relevance

#### ## Task

You are a professional DocVQA quality evaluation expert. Your task is to evaluate whether the PDF screenshots referenced in the answer can effectively support the corresponding answer content. You need to determine whether the visual information (text, charts, data) in the screenshots is consistent with the facts mentioned in the answer.

You will receive a question, a standard answer (without images), and the model's generated answer with interleaved images.

#### ## Evaluation Dimensions

- Truthfulness: Does the screenshot contain the key data or descriptions mentioned in the answer?
- Sufficiency: Does the screenshot provide sufficient evidence for the conclusion, or is it taken out of context?
- Localization Accuracy: Does the screenshot precisely cover the answer source, or does it contain irrelevant information?
- Alignment: Does the screenshot exactly match the text being cited? Any misalignment is a flaw.

#### ## Scoring Criteria

**\*\*BE STRICT. A score of 5 is extremely rare and requires perfection. Most good answers should score 3-4.\*\***

- 0: No support at all. The screenshot content is completely irrelevant to the answer.
- 1: Extremely weak support. The screenshot only mentions vague related concepts without specific data.
- 2: Weak support. The screenshot contains partial key data, or has significant quality issues.
- 3: Moderate support. The screenshot covers most of the evidence but has flaws (e.g., includes irrelevant content, slight misalignment with cited text, or captures too much/too little).
- 4: Good support. The screenshot contains the core evidence with minor flaws. This is where most correct answers should score.
- 5: **\*\*PERFECT support (extremely rare)\*\***. The screenshot must be **\*\*flawless\*\***: precise bounding box that exactly covers the cited text, no extra content, no skewing, no misalignment, and the evidence perfectly matches what is claimed. **\*\*Only give 5 when every single detail is perfect.\*\***

#### ## Important Notes

- Be conservative with scores. If you hesitate between two scores, choose the lower one.
- A slightly off-center crop, a small amount of extra content, or minor misalignment = score 3-4, NOT 5.
- Score 5 should only be given when the bounding box is pixel-perfect and the evidence is exactly what was cited.

#### ## Output Format

Please output two lines for the results: the first line is your reasoning for the score, and the second line is the score. Strictly follow this format without any additional content.

#### # Output Example

A reason why you choose this score (from 0 to 5).  
```<relevance\_score>X</relevance\_score>```

### Prompt for Evaluating Answer Correctness

#### ## Task

You are a multimodal QA evaluation expert. Your task is to evaluate the overall quality of the answer. Provide your evaluation in the form of "reasoning" and "score". Evaluation should be based solely on the standard answer, without introducing your own external knowledge.

You will receive a question, a standard answer, and the model's generated answer.

#### ## Evaluation Criteria

**\*\*BE STRICT. Most answers are not as good as they appear. When in doubt, choose the lower score.\*\***

- 0 (Completely Unsolved): The answer is completely off-topic or directly contradicts the standard answer.
- 1 (Mostly Unsolved): The answer has extremely low relevance, providing almost no valuable information.
- 2 (Partially Solved): The answer covers some aspects but misses key information or has obvious factual errors. **\*\*Many "okay" answers fall here - do not over-rate.\*\***
- 3 (Acceptable): The answer covers the core facts but is incomplete, lacks necessary details, or has minor errors. **\*\*Only give this when the answer is genuinely useful despite clear gaps.\*\***
- 4 (Good): The answer clearly covers all key points with rigorous logic. Near-complete and accurate. **\*\*Reserve for strong answers. Do not hand out freely.\*\***
- 5 (Excellent): Complete, accurate, and perfectly structured and the answer must not be significantly more verbose than the standard answer. **\*\*Extremely Difficult to reach. Do not give 5 unless truly perfect in every dimension.\*\***

#### ## Important Notes

- Ignore phrases like "cited from" or "from" that may appear in the model's generated answer - they are irrelevant.
- **\*\*DO NOT penalize the answer based on the language it is written in.\*\*** Chinese, English, or mixed - score the content only.
- Only the exact facts in the standard answer count. Extra details beyond the standard answer do NOT improve the score.

#### ## Output Format

Please output two lines for the results: the first line is your reasoning for the score, and the second line is the score. Strictly follow this format without any additional content.

#### # Output Example

A reason why you choose this score (from 0 to 5).  
```<qa\_acc>X</qa\_acc>```

## F Limitations & Potential Negative Impacts

**Limitations** While CiteVQA introduces a rigorous framework for traceable document intelligence, it entails certain inherent trade-offs. First, although the benchmark spans seven major domains, the definition of authoritative evidence may involve domain-specific nuances in highly specialized vertical fields that warrant further exploration. Second, our automated curation pipeline prioritizes data fidelity by leveraging state-of-the-art Multimodal Large Language Models (MLLMs), which, while ensuring high-quality reasoning and attribution, introduces a significant computational resource barrier for large-scale replication. Finally, the multi-dimensional evaluation protocol—incorporating coordinate verification and fine-grained textual alignment—requires higher computational overhead compared to standard VQA tasks, representing a deliberate choice to prioritize evaluative depth and traceability over raw scoring efficiency.

**Potential Negative Impacts** A potential negative impact is the risk of models overfitting to the specific metrics and document distributions of CiteVQA. While our benchmark aim to improve document intelligence, excessive optimization for these specific tasks may lead to reduced generalizability when models encounter diverse real-world document structures not represented in our dataset.